

COMPARISON STUDIES OF DOWEX MSA-1 RESIN AND SCOTT
IMPREGNATED CHARCOAL FOR IODINE ADSORBENTS
IN AN IODINE AIR MONITOR SYSTEM

by

DANIEL GEORGE GREEN

B.S., KANSAS STATE UNIVERSITY, 1980

A MASTER'S THESIS

submitted in partial fulfillment of the
requirements for the degree


MASTER OF SCIENCE

Department of Nuclear Engineering

KANSAS STATE UNIVERSITY
Manhattan, Kansas

1981

Approved by:


Major Professor

**THIS BOOK
CONTAINS
NUMEROUS PAGES
WITH THE ORIGINAL
PRINTING BEING
SKEWED
DIFFERENTLY FROM
THE TOP OF THE
PAGE TO THE
BOTTOM.**

**THIS IS AS RECEIVED
FROM THE
CUSTOMER.**

SPEC
COLL
LD
2668
T4
1981
G73
C. 2

A11200 067964

1

TABLE OF CONTENTS

	<u>Page</u>
1.0 Introduction	1
2.0 Resin and Charcoal Characterization	5
2.1 General	5
2.2 Physical Adsorption and Chemisorption	5
2.3 Dowex MSA-1 Resin	6
2.4 Resin Porosity and Surface Area	9
2.5 Charcoal.	10
2.6 Cost Comparison	12
3.0 Theory	13
3.1 NAA Theory.	13
3.2 Standard Curve.	19
3.3 Physical Geometry	20
3.4 Net Analyzer Response for Gamma-Ray Photopeaks.	20
3.5 NAA Reactions of Interest	21
3.6 Computer Programs	21
3.7 Collection Efficiency	24
4.0 Experimental Procedures.	25
4.1 Iodine Sampling System.	25
4.2 Method of Iodine Collection	27
4.3 Production of Radioactive Iodine.	29
4.4 Determination of Iodine Content and Computer Analysis of Pulse Height Distributions.	30
4.5 Standard Curve.	34
4.6 Experimental Conditions Investigated.	34
4.6.1 Temperature	35
4.6.2 Air Flow Rate.	35
4.6.3 Retention.	36
4.6.4 Incident Mass of Iodine.	37
4.6.5 Humidity	37
4.6.6 Radon and Thoron Collection.	39
5.0 Results and Conclusions.	41
5.1 Mass of Iodine Collected	41
5.2 Elevated Temperatures.	41
5.3 Air Flow Rate.	44
5.4 Mass of Incident Iodine.	44
5.5 Post Collection Heating.	47
5.6 High Humidity.	47
5.7 Radon and Thoron Collection.	51
5.8 Conclusion Summary	52

TABLE OF CONTENTS (Continued)

	<u>Page</u>
6.0 Recommendations	54
7.0 Acknowledgements	56
8.0 References	58
9.0 Appendix A: Standard Deviation Derivation	59
10.0 Appendix B: CL - SUBT List.	68
11.0 Appendix C: FDC List.	76
12.0 Appendix D: Raw Data.	79

LIST OF FIGURES

<u>Figure</u>	<u>Page</u>
2.1 Pulse height distribution resulting from gamma-ray decay of the activated components of a neutron irradiated resin sample	8
2.2 Pulse height spectrum resulting from gamma-ray decay of the neutron activated components of an irradiated charcoal sample.	11
3.1 The time dependence of the number of activated nuclei in a sample, where the sample is irradiated up to time t_i and then the activated nuclei are allowed to decay starting at t_r	14
4.1 Diagram of the adsorption column, illustrating the dimensions and the construction of this column, using polypropylene and fine mesh stainless steel screens	26
4.2 The iodine sampling system showing the dimensions and location of each of the components.	28
4.3 The Canberra Series 80 Multichannel Analyzer and the Germanium Lithium-drifted detector system used for data collection after sample irradiation.	31
4.4 The configuration used for counting the resulting gamma rays from the activated ^{128}I present in the sample vials.	32
4.5 The iodine sampling system used for the humidity study, illustrating the dimensions and location of each of the system's components	38
5.1 Graph of the linear relationship between the measured sample counting rate resulting from the ^{128}I gamma-ray decay, and the iodine mass present in the sample.	42
5.2 Charcoal adsorption column efficiency versus the mass of iodine incident on the column, under high humidity conditions (columns saturated with water)	49
5.3 Resin adsorption column efficiency versus the mass of iodine incident on the column, under high humidity conditions (columns saturated with water).	50
5.4 Pulse height distribution resulting from gamma-ray decay of thoron daughter products collected on the particulate filter papers	53

LIST OF FIGURES (Continued)

<u>Figure</u>	<u>Page</u>
A.1 Representation of a typical pulse height spectrum for an irradiated resin sample which did not contain iodine.	60
A.2 Illustration of the pulse height distribution for an irradiated resin sample containing iodine.	61

LIST OF TABLES

<u>Table</u>	<u>Page</u>
3.1 Data for radioisotopes produced by neutron activation in the KSUTMII nuclear reactor, and used for the neutron activation analysis of the samples	22
5.1 Experimental data for adsorption column collection efficiencies, for both resin and charcoal, at varying temperatures	43
5.2 Experimental data for adsorption column collection efficiencies, for both resin and charcoal, at varying air flow rates	45
5.3 Experimental data for resin and charcoal adsorption column efficiencies for various incident iodine masses.	46
5.4 Experimental data for the retention of adsorbed iodine on resin or charcoal at various temperatures.	48
D-I Data for the reference iron wire flux monitor.	80
D-II Data for the standard curve, illustrating the relationship between ^{128}I counting rate and the mass of iodine present in the sample.	81
D-III Data showing the counting rate of the ^{128}I present on the resin before heating in the retention study.	82
D-IV Data showing the counting rate of ^{128}I present on the resin after heating in the retention study	83
D-V Data showing the counting rate of ^{128}I present on the charcoal before heating in the retention study	84
D-VI Data showing the counting rate of ^{128}I present on the charcoal after heating in the retention study.	85
D-VII Data collected during the humidity study with resin as the adsorbent material	86
D-VIII Data collected during the humidity study with charcoal as the adsorbent material	87
D-IX Data obtained during the elevated temperature experiment with the charcoal adsorbent material	88
D-X Data obtained during the elevated temperature experiment with the resin adsorbent material.	89

LIST OF TABLES (Continued)

<u>Table</u>		<u>Page</u>
D-XI	Data obtained during the air flow rate study with the charcoal adsorbent material	90
D-XII	Data obtained during the air flow rate study with the resin adsorbent material.	91
D-XIII	Data collected which yielded the results of the incident iodine mass study with charcoal adsorbents.	92
D-XIV	Data obtained which yielded the results of the incident iodine mass study with resin adsorbents	93

1.0 INTRODUCTION

Radiological monitoring of airborne radioiodine is required to determine the dose received by individuals performing experiments utilizing radioactive iodine and by individuals at nuclear power reactor facilities. This necessitates measurement of the concentration of radioiodine in the laboratory and in the environment at nuclear power plant sites. Presently, radioiodine levels are measured using three basic types of iodine air samplers, these are :^{1,2}

(1) a total iodine and particulate air sampler utilizing a particulate filter and a charcoal cartridge, (2) an iodine molecular species differentiating air sampler containing in series, a particulate filter, a cadmium iodide bed, a bed of 4-iodophenol absorbed on alumina, and a silver zeolite or impregnated charcoal bed, and (3) a total iodine air sampler consisting of a charcoal-impregnated filter paper.

Investigation of an alternate iodine air sampler that considers both laboratories and nuclear reactors as areas of application is required.

The expanding use of ^{125}I in research laboratories has logically increased the risk for workers in these facilities of inhaling airborne radioactive iodine. Researchers involved in using radioiodine for labeling organic compounds include persons in the fields of veterinary science, biochemistry, and biology. Inhalation of radioactive iodine will ultimately lead to accumulation of this iodine in the thyroid. Risk of this occurrence necessitates that a thyroid scan be performed within 7 days after any researcher has worked with ^{125}I at Kansas State University and other research institutions. This after the fact method of controlling exposure is not the preferred technique. The preferred

method is that of continuous monitoring during the time period the radioiodine is being used in the laboratory. This would provide an instantaneous indication of the radiation level and allow control of the airborne iodine concentrations. Because of the extremely low concentration of the radioactive gas in the air, the radioiodine must first be concentrated by flowing air through a cartridge containing material which has a high affinity for iodine. Therefore, in order to measure the concentration of airborne radioactive iodine, a reliable air sampler is needed to collect this iodine.

This radioiodine air sampler would also be applicable for environmental monitoring around nuclear power reactors and research reactors. During normal reactor operations or, to a greater extent, during an accident situation, the release of radioactive material to the environment poses an inherent hazard. Under these circumstances the major risk to the general public is due to the volatile components of the released materials such as the fission products of iodine isotopes. Therefore, routine monitoring of the airborne concentrations of ^{129}I , ^{131}I and ^{135}I are very important at nuclear reactors. The radioiodine in the gaseous effluents from a nuclear reactor may be in either particulate or gaseous form. Moreover, these forms³ may be elemental iodine (I_2), inorganic iodides (principally HOI), and organic iodides (predominately CH_3I). Presently, activated and impregnated charcoals and silver zeolite are used as air samplers in these situations. However, according to Hassler⁴, organic iodides are not adsorbed on activated charcoal, which indicates that methyl iodide and other iodides cannot be monitored accurately using this charcoal. Also, activated charcoal's ability for

iodine adsorption is reduced under high humidity conditions. Iodine adsorption capabilities under high humidity conditions may be improved through the use of silver zeolite or charcoal impregnated with potassium iodide or triethylenediamine. The silver zeolite adsorbs iodine as well as the impregnated charcoal, however, presently the silver zeolite's cost is 10 times that of the impregnated charcoal's cost.⁵ An additional problem with the charcoals, either impregnated or unimpregnated, is that when they are used as an air sampler they will collect other radionuclides such as xenon.⁶

Some research reactors use gross gamma-ray counting of all radionuclides collected on a charcoal impregnated filter paper as the air sampler on their iodine monitors. Monitors of this type are sensitive to all gamma emitting radionuclides. When radon and thoron levels increase significantly, due to meteorological conditions, false alarms are triggered. This situation exists at the Kansas State University TRIGA MARK II nuclear reactor. These alarms must be evaluated carefully to insure that they were not due to an increase in airborne radioiodine.

The above described problems with charcoal and silver zeolite lead to the assumption that a better radioiodine air sampler was needed. Previous work⁷⁻⁹ showed that a strong base anion exchange resin, used in either wet or dry form, had a strong affinity for iodine and iodides. Therefore, comparison of impregnated charcoal and this resin was initiated.

The experimental procedures developed and the data obtained, during the course of this research allowed, for the first time, a comparison to be made between the efficiency of charcoal and resin filled air sampler

cartridges. Various parameters were studied to determine each parameters effect on the particular adsorption column's efficiency.¹⁰ The efficiencies for the charcoal and resin columns were determined using neutron activation analysis. This procedure consisted of collecting stable iodine (I_2) on an adsorption column, producing radioactive ^{128}I by neutron irradiation of the material in the column using the Kansas State University TRIGA Mark II nuclear reactor, and then measuring the gamma rays produced by ^{128}I decay. Comparison of the data on each parameter, for resin and charcoal, was then undertaken to determine which substance was better for use in an iodine-monitor air sampler.

2.0 RESIN AND CHARCOAL CHARACTERIZATION

2.1 General

In order to understand the relative efficiencies of triethylenediamine-impregnated activated charcoal and the resin (Dowex MSA-1) under investigation, it is important to characterize each type of material. Obviously, their physical properties and chemical compositions are quite different. An important common property is that they both collect elemental iodine by physical adsorption. However, relative efficiency data for these two materials, are non-existent. Extensive research has been performed on charcoal, hence, its characteristics are well known. Furthermore, enhanced efficiency has been achieved, through activation of charcoal to increase the surface area. Also, impregnants have been added to charcoal to allow collection of organic iodides. Conversely, minimal research, leading to improving the efficiency of resin for the collection of airborne radioiodine, has been performed.

2.2 Physical Adsorption and Chemisorption

The phenomenon of concentration of a substance on the surface of a solid is called adsorption. While it is probably true that all solids adsorb gases to a certain extent, usually adsorption is not very pronounced unless the adsorbent possesses a large surface area for a given mass. Logically with an increase in the surface area of an adsorbent there is an increase in the total amount of gas that may be adsorbed. This adsorption of gas by a solid would be accompanied by heat evolution which is termed heat of adsorption.

Physical adsorption is the term applied to the type of adsorption

in which no electrons are transferred or shared between adsorbed molecules and the adsorbent surface. Physical adsorption is also characterized by low heats of adsorption. This type of adsorption is caused by van der Waal's forces, which are also responsible for causing vapor molecules to condense to a liquid. Similarly, in physical adsorption, as in the condensation of a gas, the attachments are weak.

Chemisorption involves the formation of a chemical compound between the adsorbed gas and the surface material. Therefore, unlike physical adsorption, electrons may be transferred or shared between the adsorbed molecules and the adsorbent surface. The attachments in chemisorption are also stronger than those in physical adsorption. Also, whereas physical adsorption was characterized by low heats of adsorption, chemisorption may be characterized by much higher heats of adsorption.

2.3 Dowex MSA-1 Resin

Dowex MSA-1 resin was chosen for this study. This particular resin was selected because its chemical composition is similar to another strong anion exchange resin. The similar resin, Dowex 1-X8, possesses a high affinity, in wet or dry form, for iodine and organic iodides. However, Dowex MSA-1 was selected for the subject air sampler since dehydrated MSA-1 has a higher porosity and hence, has more internal surface area ($23 \text{ m}^2/\text{g}$) for the adsorption of iodine. Conversely, the Dowex 1-X8 resin is a gel and will collapse upon removing the moisture. Since resins have a range of particle sizes, quoted values are averages. The U.S. standard mesh size range of the Dowex MSA-1 anion exchange resin is 20-50 and has an average particle diameter of 0.57 mm. The wet density of this resin is 0.67 g/m^3 and the moisture content is 60%. This resin is received from the supplier packaged in water. For this

study, the water was removed so that more adsorption sites would be available to adsorb iodine.

The dehydration procedure¹¹ for this resin was to first displace the water in the resin with methanol. This was done by placing 1 part of resin into 2 parts of methanol. This solution was then mixed vigorously. Next, the resin was allowed to soak in the methanol for 12 hours. The resin was then dried at a temperature below 50°C using a Fisher Infra-Radiator heat lamp for 3 hours.

Dry resin samples were irradiated in the TRIGA Mark II nuclear reactor to determine if significant radionuclide production resulted. The pulse height distribution of an irradiated resin sample is shown in Fig. 2.1. This figure clearly indicates that one of the components of the resin was chlorine. The significance of the chlorine is discussed in section 3.6 .

The major problem associated with handling the resin was its adherence to everything. This was due to static electricity generated as the resin was poured from one container to another. The problem was solved through the use of an electrically grounded metal funnel and grounded metal pans.

Previous work indicated that anion exchange resins would physically adsorb iodine vapor. For example, in 1961, it was reported by B. Sansoni⁷ that 3.4 g of iodine could be physically adsorbed by 1 g of an anion exchange resin. Also, in 1966, it was indicated by A.V. Nikolaev, et.al.⁸, that iodine vapors were adsorbed by an anion exchange resin. They attributed the sorption-mechanism to physical adsorption by the resin matrix. As a result of these studies, it appears that physical adsorption is the mechanism by which iodine is collected by the resin.

**THIS BOOK
CONTAINS
NUMEROUS PAGES
WITH DIAGRAMS
THAT ARE CROOKED
COMPARED TO THE
REST OF THE
INFORMATION ON
THE PAGE.**

**THIS IS AS
RECEIVED FROM
CUSTOMER.**

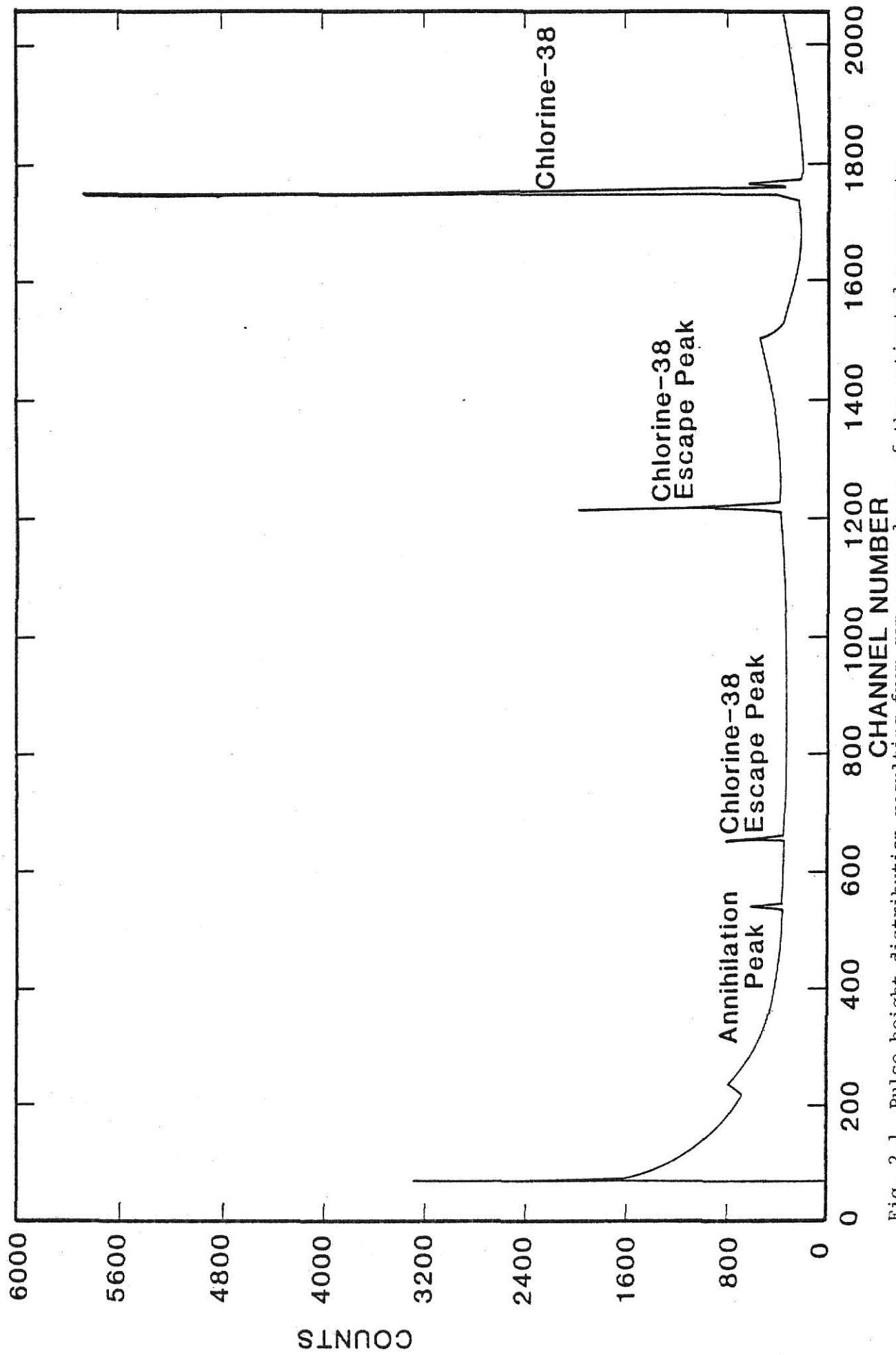


Fig. 2.1 Pulse height distribution resulting from gamma-ray decay of the activated components of a neutron irradiated resin sample.

2.4 Resin Porosity and Surface Area

Since the particles of Dowex MSA-1 are spherically shaped, the average wet particle mass m_w may be found using

$$m_w = (4/3 \pi r_w^3) \rho_w , \quad (2.1)$$

where r_w is the average wet particle radius, and ρ_w is the wet particle density. The data for moisture content was then utilized to yield

$$\% \text{ moisture content} = \frac{m_w - m_d}{m_w} \times 100\% , \quad (2.2)$$

where m_w is defined above and m_d is the dry particle mass. Rearranging Eq. (2.2) gives

$$m_d = m_w \frac{(100 - \% \text{ moisture content})}{100} . \quad (2.3)$$

Now, upon dehydration, the resin volume is reduced¹¹ such that

$$V_d = 0.97 V_w , \quad (2.4)$$

where V_d is the volume of the dry resin and V_w is the volume of the wet resin. Using Eqs. (2.3) and (2.4), the dry resin density is

$$\rho_d = m_d / V_d . \quad (2.5)$$

The pore volume of the dehydrated resin particle V_g is now found using the relation¹²

$$V_g = \Theta \rho_d , \quad (2.6)$$

where Θ is the porosity of the resin and ρ_d is the dry particle density.

The average pore radius r_p may then be calculated using the relation¹²

$$r_p = 2V_g / S_g \quad (2.7)$$

where S_g is the internal pore surface area.

The external surface area S is found by subtracting the total pore mouth area A_{pore} from the surface area of a sphere of the same radius containing no pores¹³

$$A_{\text{pore}} = A \left(\frac{1}{\sqrt{2}} \right) \quad (2.8)$$

where A is the surface area for a sphere with radius r_d . Hence,

$$S = 4\pi r_d^2 - 4\pi r_d^2 \frac{1}{\sqrt{2}} \quad (2.9)$$

where r_d is the dry resin sphere radius and may be found from Eq. (2.4).

The total surface area may now be found by adding the result of Eq.

(2.9) and S_g . Using the above equations and data provided by Dow Chemical Company, yields the following results for dehydrated Dowex MSA-1 resin; porosity equals 20%, a total surface area of $23 \text{ m}^2/\text{g}$, and ignition temperature at 230°C .

2.5 Charcoal

The charcoal used in this study was manufactured by North American Carbon. It was designed for the removal of radioactive iodine and organic iodides from steam-air mixtures below 200°C . The surface area, both internal and external, is $1000 \text{ m}^2/\text{g}$ and the density is $0.55 \text{ g}/\text{m}^3$. Therefore, using these and other data supplied by Scott Health and Safety Products¹⁴ and Eq. (2.6) yields the following results; a porosity of 30% and ignition temperature at 300°C . This coconut charcoal is impregnated with triethylenediamine (TEDA) and potassium iodide. The iodide of the potassium iodide was indicated from the pulse height spectrum of an irradiated charcoal sample (See Fig. 2.2.)

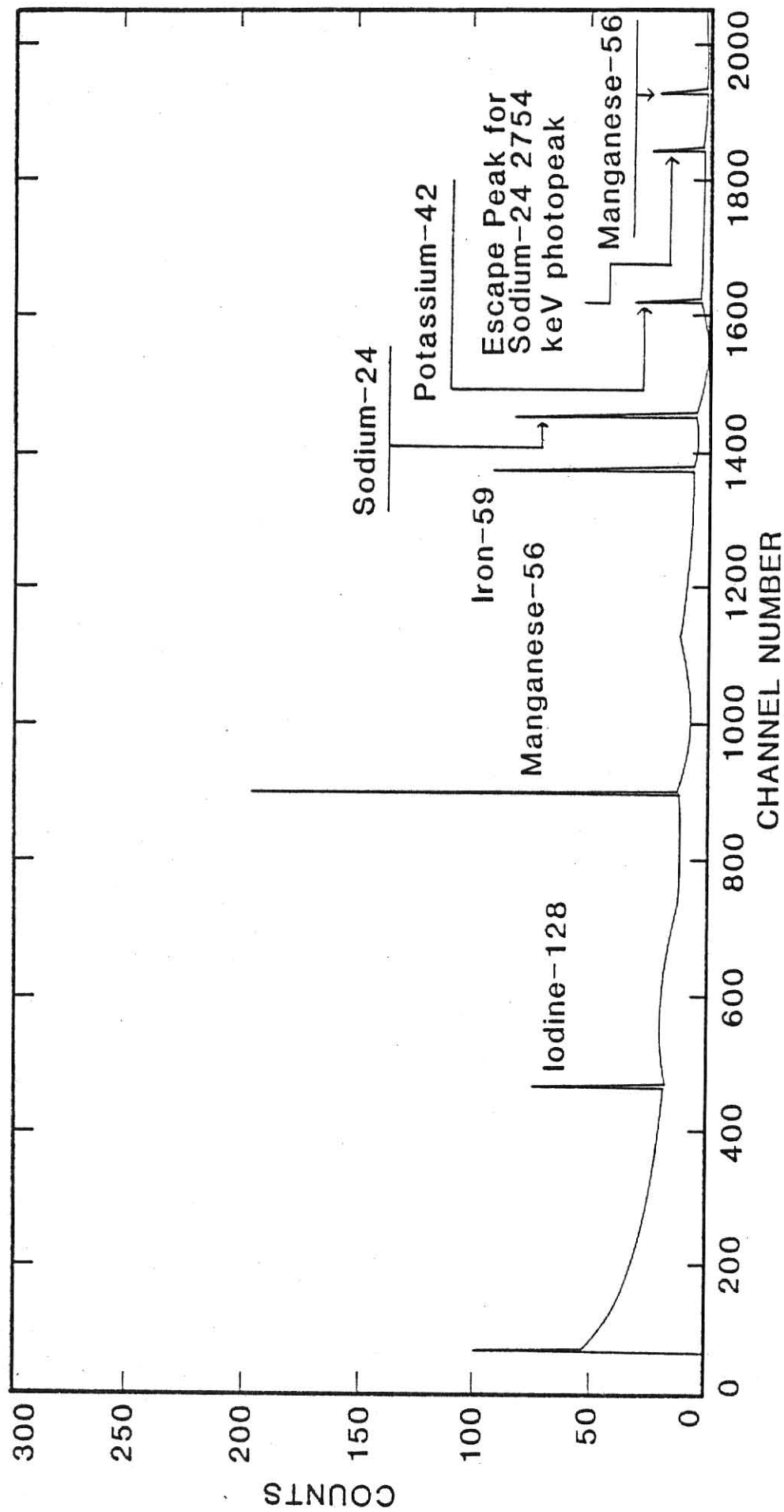


Fig. 2.2. Pulse height spectrum resulting from gamma-ray decay of the neutron activated components of an irradiated charcoal sample.

However, this amount was small when compared to the amount of iodine added to the charcoal column during a typical adsorption study.

Elemental iodine (I_2) is physically adsorbed¹⁵ on activated charcoal surfaces regardless of any impregnation. However, the potassium iodide was added to the charcoal to chemisorb organic iodides by the reaction¹⁶

$$CH_3^{131}I + ^{127}I(\text{on charcoal}) \rightarrow CH_3^{127}I + ^{131}I(\text{on charcoal}),$$

where $CH_3^{131}I$ is used as the typical organic iodide.

The TEDA was also added to the charcoal to chemisorb organic iodides, however, as a group, amines are more receptive to methyl iodide molecules than to water molecules¹⁵, therefore higher collection efficiencies for this type of charcoal should occur.

2.6 Cost Comparison

Lastly, a cost comparison between a 4 ml adsorption column of impregnated charcoal and one of resin indicates that charcoal is more cost effective. The price of a Dowex MSA-1 resin column supplied by Xentex, Inc. of Kansas City is \$0.056 while the price of an impregnated charcoal column supplied by HI-Q Filter Products Company is \$0.028.

3.0 THEORY

The iodine collection efficiency of charcoal and resin adsorbent samples was determined using Neutron Activation Analysis (NAA). NAA is the process by which a radionuclide may be identified by its characteristic gamma-ray emissions.

To interpret data from neutron activation, a number of parameters must be considered. These are: neutron flux variations during irradiation, irradiation time, decay time and counting time, as well as counting geometry, and the net analyzer response for a gamma-ray photopeak.

3.1 NAA THEORY

For an irradiated sample, the number of nuclei N_0 activated during irradiation, can be represented by¹⁷

$$N_0 = \frac{\sum_a \phi}{\lambda} (1 - e^{-\lambda t_r}) \quad , \quad (3.1)$$

where \sum_a is the macroscopic absorption cross section, ϕ is the neutron flux, λ is the decay constant, and t_r is the activation time. Now, as shown in Fig. 3.1, the gamma-ray photopeak area that results for a counting time t_1 corrected for background, is

$$\text{Area} = (N_1 - N_2)(\text{eff})(\% \gamma)(\text{PCT}), \quad (3.2)$$

where N_1 is the number of radioactive nuclei present at time t_d (decay time of the sample), N_2 is the number of radioactive nuclei present at

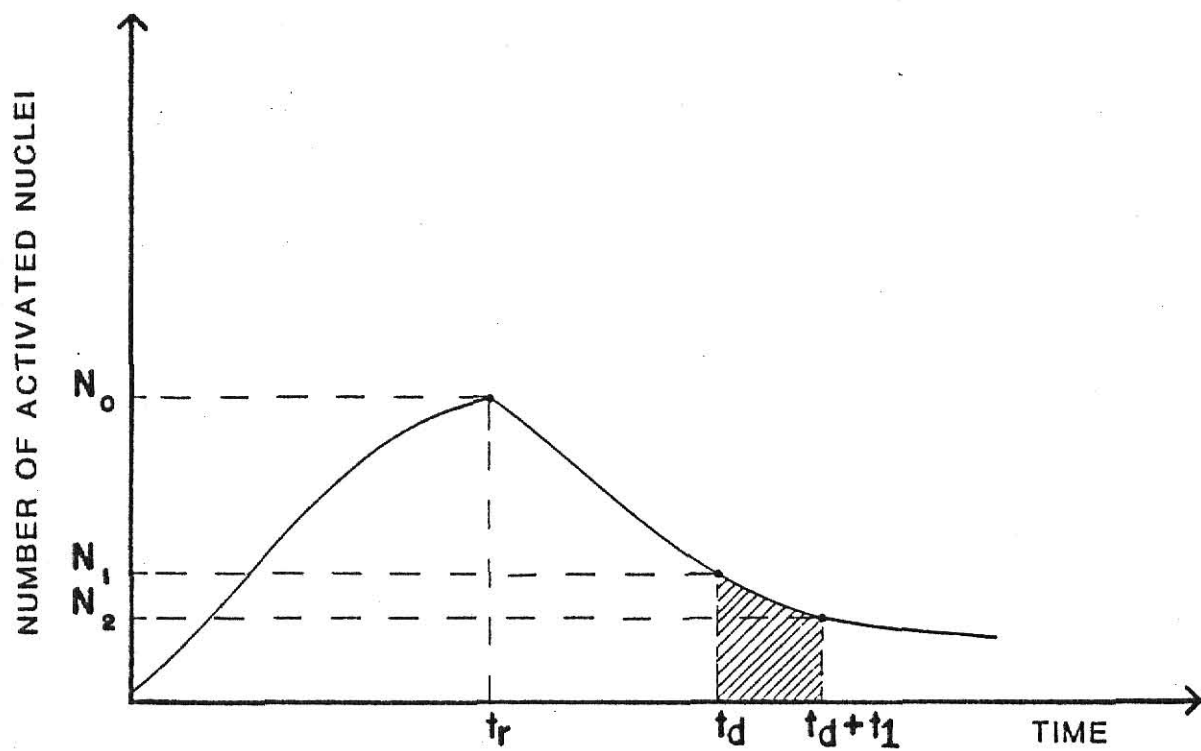


Fig. 3.1. The time dependence of the number of activated nuclei in a sample, where the sample is irradiated up to time t_r and then the activated nuclei are allowed to decay starting at t_r .

time $t_d + t_1$, eff is the overall detection efficiency, % γ is the gamma yield, and PCT is the percent abundance of the isotope. Then, using the decay equation,

$$N = N_0 e^{-\lambda t_d}, \quad (3.3)$$

and substituting Eq. (3.3) into Eq. (3.2) gives

$$\text{Area} = (N_0 e^{-\lambda t_d} - N_0 e^{-\lambda(t_d + t_1)}) (\text{eff}) (\% \gamma) (\text{PCT}) . \quad (3.4)$$

Rearranging Eq. (3.4) and solving for N_0 yields

$$N_0 = \frac{\text{Area}}{e^{-\lambda t_d} (1 - e^{-\lambda t_1}) (\text{eff}) (\% \gamma) (\text{PCT})} . \quad (3.5)$$

Substitution of Eq. (3.1) into Eq. (3.5) results in

$$\frac{\sum_a \phi}{\lambda} (1 - e^{-\lambda t_r}) = \frac{\text{Area}}{e^{-\lambda t_d} (1 - e^{-\lambda t_1}) (\text{eff}) (\% \gamma) (\text{PCT})} . \quad (3.6)$$

However, writing \sum_a in terms of mass, so that this unknown quantity (mass) may be specified in terms of known values, yields

$$\sum_a = \frac{M}{\text{Vol } A} (6.023 \times 10^{23}) (\sigma_a) \quad (3.7)$$

where σ_a is the microscopic absorption cross section, A is the atomic number of the parent nuclei, and M/Vol is the density of the parent nuclei. Substituting Eq. (3.7) into Eq. (3.6) and solving for the mass of the parent nuclei gives

$$M = \frac{Vol A \lambda Area}{(6.023 \times 10^{23}) \sigma_a \phi (1 - e^{-\lambda t_r}) (e^{-\lambda t_d}) (1 - e^{-\lambda t_l}) (eff) (\% \gamma) (PCT)} , \quad (3.8)$$

which is the mass of the parent nuclei that is converted to the radionuclide during time t_r . The rate of production of the radionuclide for two samples differing only in mass would be the same if self shielding effects are neglected. Therefore, the mass ratio of the isotopic sample (a) and the reference sample (ref), irradiated for the same time period, is

$$\frac{M_a}{M_{ref}} = \frac{\frac{(Vol)_a A \lambda (Area)_a}{(6.023 \times 10^{23}) \sigma_a \phi_a (1 - e^{-\lambda t_r}) (e^{-\lambda t_{da}}) (1 - e^{-\lambda t_{la}}) (eff) (\% \gamma) (PCT)}}{\frac{(Vol)_{ref} A \lambda (Area)_{ref}}{(6.023 \times 10^{23}) \sigma_{ref} \phi_{ref} (1 - e^{-\lambda t_r}) (e^{-\lambda t_{dref}}) (1 - e^{-\lambda t_{lref}}) (eff) (\% \gamma) (PCT)}}} . \quad (3.9)$$

Cancellation of the common terms in Eq. (3.9) gives the general equation for mass ratios

$$\frac{M_a}{M_{ref}} = \frac{\phi_{ref} (Area)_a e^{-\lambda t_{dref}} (1 - e^{-\lambda t_{lref}})}{\phi_a (Area)_{ref} e^{-\lambda t_{da}} (1 - e^{-\lambda t_{la}})} . \quad (3.10)$$

Since the samples are counted for the same live time (t_1), Eq. (3.10) reduces to

$$\frac{M_a}{M_{ref}} = \frac{\phi_{ref} (Area)_a}{\phi_a (Area)_{ref}} \frac{e^{\lambda t_{da}}}{e^{\lambda t_{dref}}} \quad (3.11)$$

Rearranging Eq. (3.11) gives

$$\frac{\phi_a}{\phi_{ref}} = \frac{M_{ref} (Area)_a}{M_a (Area)_{ref}} e^{\lambda(t_{da} - t_{dref})} \quad (3.12)$$

Equation (3.12) may then be used to account for variations in the neutron flux. The quantity ϕ_a/ϕ_{ref} is measured by attaching iron wires to the irradiation sample vials, and then irradiating these vials. Therefore,

$$\frac{\phi_a}{\phi_{ref}} = \frac{\phi_{wa}}{\phi_{wref}} \quad (3.13)$$

where ϕ_w , the neutron flux used to activate an iron wire, is

$$\phi_w = \frac{(Vol)_w \lambda_w (Area)_w}{M_w (6.023 \times 10^{23}) \sigma_{aw} (1 - e^{-\lambda_w t_r}) (e^{-\lambda t_{dw}}) (eff) (\% \gamma) (PCT) (1 - e^{-\lambda t_{lw}})} \quad (3.14)$$

Therefore, using the same assumptions as stated for Eqs. (3.9), (3.13), and (3.14) gives

$$\frac{\phi_a}{\phi_{ref}} = \frac{\phi_{wa}}{\phi_{wref}} = \frac{M_{wref}}{M_{wa}} \frac{(Area)_{wa}}{(Area)_{wref}} e^{\lambda_w(t_{dwa} - t_{dwref})} \quad (3.15)$$

Equation (3.15) may then be used to correct for neutron flux variations for a given isotope sample with respect to a known reference sample.

The correction for radioactive decay may be found after multiplying Eq. (3.3) by the decay constant. The resulting factor, λN , is simply the activity of the sample. However, since the activity is proportional to the counting rate, the resulting equation may then be written as

$$C = C_0 e^{-\lambda t_d}, \quad (3.16)$$

where C is the counting rate of the sample at the time t_d , (the decay time and half of the count time) and C_0 is the counting rate of the sample before decay has occurred. Rewriting Eq. (3.16) yields

$$C_0 = C e^{\lambda t_d}, \quad (3.17)$$

which is the equation used to correct for radioactive decay.

3.2 Standard Curve

A standard curve was used to determine the mass of the iodine present in a sample from the measured counting rate resulting from the iodine. Multiplying Eq. (3.1) by the decay constant and substituting Eq. (3.7) into Eq. (3.1) yields the initial activity of the radionuclide,

$$A_o = N_o \lambda = \frac{M}{Vol A} (6.023 \times 10^{23}) \phi (1 - e^{-\lambda t_r}) \quad (3.18)$$

Hence, from Eq. (3.18) and the fact that the counting rate is proportional to the activity,

$$C_o = j k M \quad (3.19)$$

where M is the mass of the parent nuclei, C_o is the initial counting rate of the radionuclide, j is a proportionality constant, and

$$K = \frac{\phi}{Vol A} (6.023 \times 10^{23}) (1 - e^{-\lambda t_r})_{eff} \quad (3.20)$$

Therefore, Eq. (3.19) indicates that there is a linear relation between the initial counting rate of a particular radionuclide and the mass of the parent nuclei. Using the information given above, the relationship between initial counting rate of the radionuclide and the mass of the parent nuclei was found by first activating varying amounts of the parent nuclei of interest and then analyzing the samples to determine the counting rate of these samples. After correcting for neutron flux

variations and radioactive decay, a least squares line fit was then applied to the data to determine the relationship between counting rate and mass of the particular parent nuclei.

3.3 Physical Geometry

The physical geometry of the irradiated sample is an important parameter to be considered in obtaining the pulse height distribution. The reason for this fact is that systematic experimental errors may be introduced by changing the over-all efficiency of the counting system for detecting the gamma rays emitted from the sample. Therefore, it is important that the samples be prepared consistently. Each sample was homogeneous, had the same volume and shape, and the gamma rays from the neutron activation were counted with each sample in the same position relative to the active volume of the detector.

3.4 Net Analyzer Response for Gamma-Ray Photopeaks

The net analyzer response for any gamma-ray photopeak in a germanium lithium-drifted detector pulse height distribution is the total area under the peak minus the background counts. The background is determined by averaging the number of counts in K channels on each side of the peak region. These averages are defined as background grounds \bar{B}_B and \bar{B}_A . The following equation was used to determine the net analyzer response.

$$\text{Area} = \sum_{N_c}^N C_N - \frac{N_c}{2}(\bar{B}_B + \bar{B}_A) \quad . \quad (3.21)$$

In this equation, N_c is the number of channels in the peak region and C_N is the number of counts in a particular channel of the peak region.

3.5 NAA Reactions of Interest

The neutron activation reactions of interest to this analysis were ^{56}Fe going to ^{56}Mn by the fast-neutron proton reaction, production of ^{128}I by the neutron-gamma ray reaction from ^{127}I (stable iodine). Also, as indicated in Section 2.3, one of the components of the resin was chlorine. This stable chlorine, ^{37}Cl , would then produce ^{38}Cl by a neutron-gamma ray reaction. Data for these radioisotopes are presented in Table 3.1.

3.6 Computer Programs

For a column of resin with only trace amounts of iodine adsorbed to it, the large chlorine component present in the gamma-ray pulse height distribution (See Fig. 2.1) could induce considerable error when using Equation (3.21). In order to correct this problem a computer program, CL-SUBT, was devised to subtract the chlorine component from the pulse height distribution, thereby leaving the iodine photopeak stripped of the chlorine component. In other words, the chlorine component was treated as part of the background and subtracted from the total area under the photopeak to yield the iodine gamma-ray photopeak area. This subtraction process was performed as follows. First the chlorine gamma-ray photopeak area from a pulse height distribution of the resin sample from which the chlorine component is to be subtracted was ratioed to the chlorine gamma-ray photopeak area from a pulse height distribution

Table 3.1. Data for radioisotopes produced by neutron activation in the KSUTMII nuclear reactor, and used for the neutron activation analysis of the samples.

Radionuclide	Half Life	Type of Decay	Energy (keV)	Intensity (%)
^{38}Cl	37.20 min.	Gamma-ray	1642.7	38
		Gamma-ray	2170.0	47
		Beta particle	4910.0 max	58
^{56}Mn	2.58 hr.	Gamma-ray	846.8	99
		Beta particle	2850 max	47
^{128}I	25.01 Min.	Gamma-ray	442.9	14
		Beta particle	2120.0 max	76

of a resin sample containing no iodine. These areas were found using Equation (3.21). This ratio was a normalization factor used to account for differing decay times and count times between the two pulse height distributions. Then, in order to prevent the subtraction of too much background, the normalization factor was multiplied by 0.9. The number of counts in each channel of the pulse height distribution was then multiplied by $0.9 \times$ normalization factor. The pulse height distribution resulting from the multiplication of the normalization factor was then subtracted from the pulse height distribution of the sample from which the chlorine component was to be subtracted. From the pulse height distribution resulting from the subtraction described above, the iodine gamma-ray photopeak area was calculated using Equation (3.31). The standard deviation for the iodine gamma-ray photopeak area was also calculated in CL-SUBT using the standard propagation of errors technique. A listing of CL-SUBT and derivations of the standard deviation equations used in CL-SUBT are included in Appendices B and A, respectively. Also, to insure consistent results, CL-SUBT was used on the charcoal samples. However, since chlorine was not present in the charcoal, the normalization factor was zero.

Another computer program, FDC, which corrected the iodine gamma-ray photopeak area for decay and neutron flux variations respectively, is listed in Appendix C. This program also calculated the standard deviation of the resulting counting rate using the standard propagation of errors technique.

3.7 Collection Efficiency

Once the counting rate of the iodine adsorption columns are known, using NAA to determine the ^{128}I gamma-ray counting rates of each, the column efficiencies E can then be calculated as follows,¹⁰

$$E = \left[1 - \frac{\text{"B" Column } ^{128}\text{I Counting rate}}{\text{"A" Column } ^{128}\text{I Counting rate}} \right] \times 100\% \quad (3.22)$$

As was described in Section 4.1, the "A" and "B" columns were in series with "A" being the first column on which the iodine would be incident.

4.0 EXPERIMENTAL PROCEDURES

The general experimental procedure used for this study was to develop and build a system which would collect gaseous iodine, and to then examine the effect of various parameters on this system's iodine collection performance.

4.1 Iodine Sampling System

This iodine sampling system consisted of an iodine reservoir followed in order by two adsorption columns, a paper filter holder, and an Eberline model RAS-1 vacuum pump system. The iodine reservoir was a polypropylene jar, cylindrical in shape, with a 3 inch diameter and a 5 3/8 inch length. This reservoir was connected by 4 5/8 inches of 3/8 inch diameter polypropylene tubing to the first adsorption column, "A". Column "A" was connected by 4 5/8 inches of 3/8 inch diameter polypropylene tubing to the second column, "B". These adsorption columns were constructed of 2 3/8 inch long, 1/2 inch diameter polypropylene tubing with a fine mesh stainless steel screen attached to each end of this tubing. The screens were used to hold the adsorption material in place during the study. A diagram of this column is shown in Fig. 4.1. The "B" column was connected to a paper filter holder by 3/8 inch diameter, 3 5/8 inch long polypropylene tubing. This filter holder contained a charcoal loaded paper filter during the study. This filter provided a means of determining whether iodine had managed to leak through both the "A" and "B" columns. Connected to this filter holder was the Eberline vacuum pump system. This vacuum pump system consisted of a charcoal adsorption column, to insure the pump would not

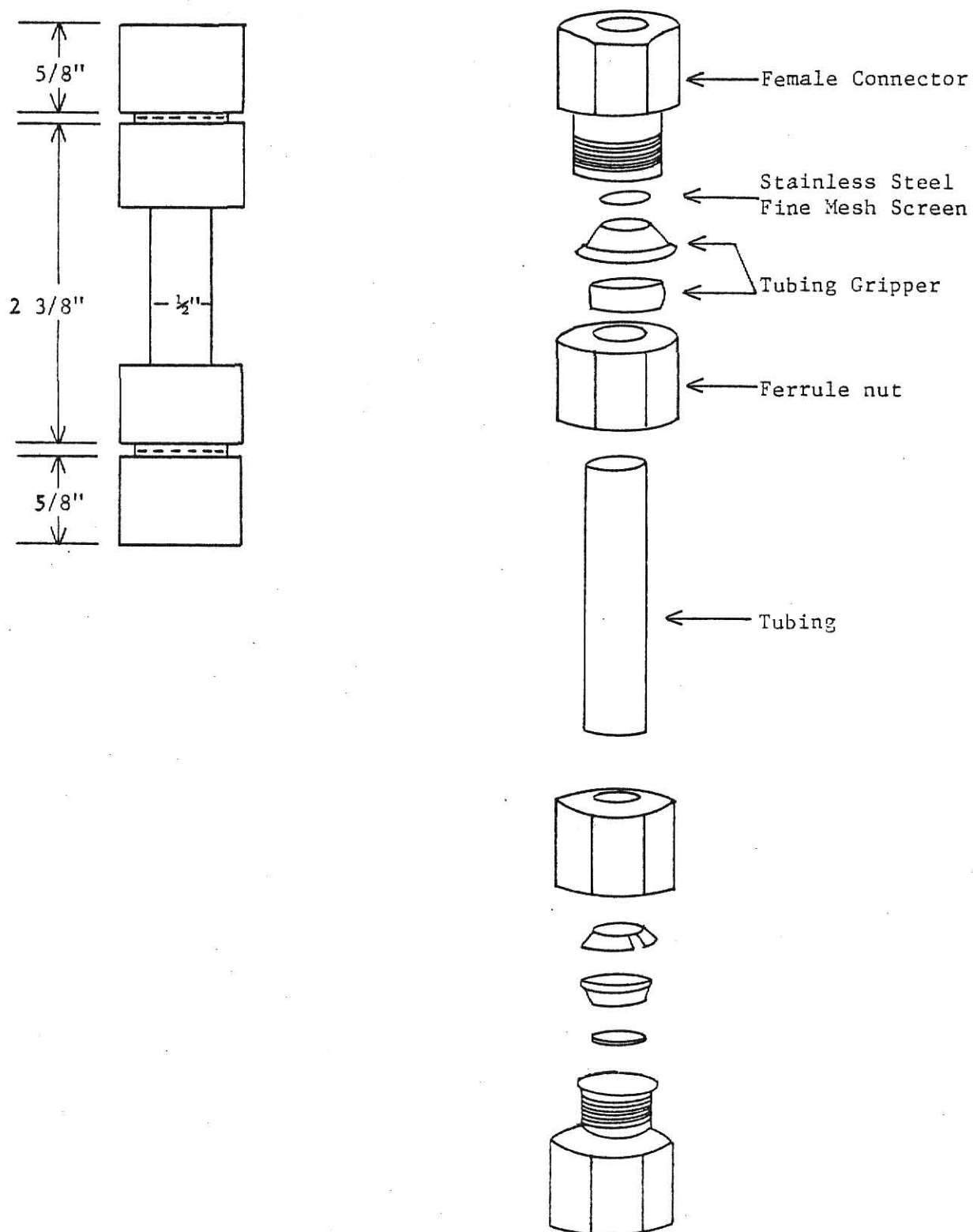


Fig. 4.1. Diagram of the adsorption column, illustrating the dimensions and the construction of this column, using polypropylene and fine mesh stainless steel screens.

be contaminated by iodine: a flow meter, used to determine gas flow rates through the system; a flow regulator to control gas flow rates; and a vacuum pump. The complete iodine sampling system is shown in Fig. 4.2.

The entire system was constructed of polypropylene since iodine will not plate out¹⁸ readily on this material. Glass is the material which iodine will plateout on the least, however, glass was deemed too difficult to work with and too fragile for a general purpose iodine sampling system. A system constructed from polyethylene was tried, but the plateout characteristics of this material were not acceptable for this study.

4.2 Method of Iodine Collection

The technique used for iodine collection, using the sampling system, was to first place a known mass of solid iodine (I_2) into the reservoir. A type H15 Mettler balance was used to measure the sample's mass. The vacuum pump was then used to draw air through the system, and consequently the iodine reservoir. As the iodine (I_2) sublimed, it was carried with the air through the system. This sublimation, the direct removal of molecules from a solid into the vapor phase, occurred because the triple point, (the point designated by the pressure and temperature at which solid, liquid, and vapor can coexist), lies well above ordinary pressures.¹⁹ This iodine gas-air mixture was carried into column "A," which was packed with either 4 ml (2.2g) of Dowex MSA-1 resin or 4 ml (2.0g) of Scott TEDA-impregnated charcoal granules. Inside the "A" column, the iodine was adsorbed as the iodine gas-air mixture passed through the column. The air and any unadsorbed iodine entered column "B", which was packed with 4 ml of resin. This second

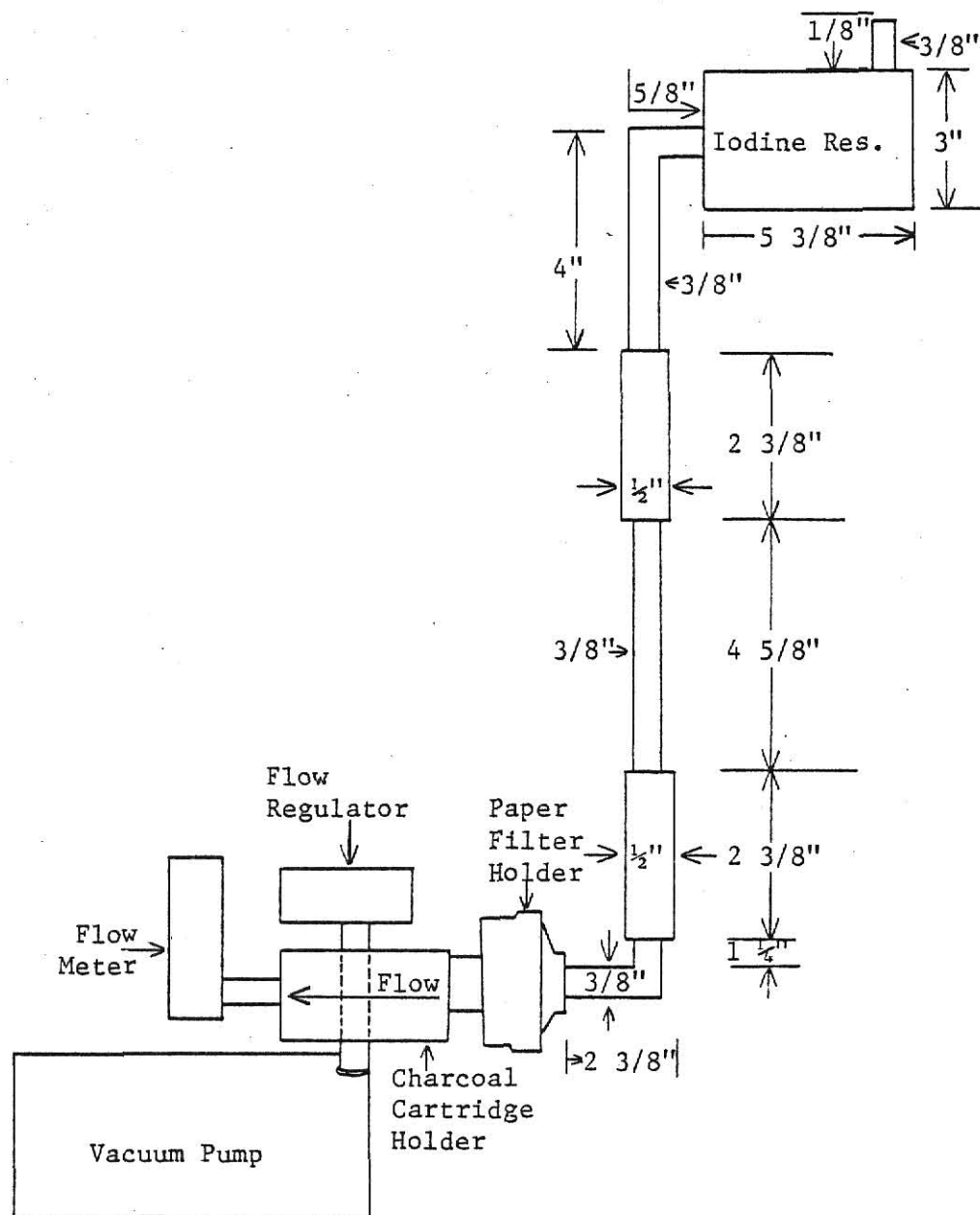


Fig. 4.2. The iodine sampling system showing the dimensions and location of each of the components.

column would then adsorb iodine from the iodine gas-air mixture as it proceeded through the "B" column. Finally, the air and any possible remaining iodine gas passed through the filter holder where the charcoal filter paper removed any small masses of remaining iodine gas that may have passed through both adsorption columns. The pump was used to draw air through the system until all of the iodine had sublimed. Once the pump was shut off, the system was dismantled and the adsorbents of each column were placed into separate grounded metal pans in order to reduce the problem of static electricity discussed in Section 2.3.

In preparation for irradiation, the adsorbents in each pan were mixed separately, and then the polypropylene and metal components of the iodine sampling systems were rinsed in methanol to remove excess iodine and then rinsed with distilled water. The homogeneous mixtures of the adsorbents and the charcoal filter paper were then each placed in the 5ml irradiation vials. The vials were polypropylene, cylindrical in shape, with a 7/16 inch diameter and a 3 inch length. To prevent the possible escape of any radioactive gases, both during and after irradiation, the vials were capped and heat sealed using a soldering iron. A Baker and Adamson 99.90% iron wires was then wrapped around each sample irradiation vial for use as a neutron flux monitor.

4.3 Production of Radioactive Iodine

These sample vials, containing adsorbents, were then irradiated to determine the iodine content of each sample using NAA. The irradiation of the sample vials was conducted in the Rotary Specimen Rack (RSR) of the Kansas State University Triga Mark II (KSUTMII) nuclear reactor.²⁰ The vials were irradiated at a power level of 10 kw for 2.5 minutes since this allowed an adequate number of iodine nuclei to be activated which could then be counted after only a short decay time.

4.4 Determination of Iodine Content and Computer Analysis of Pulse

Height Distributions

In order to determine the amount of iodine present in a sample, the samples first had to decay for a specific time. The samples were allowed to decay for one hour, so that the exposure rate required for sample removal from the KSUTMII reactor bay was in accord with the KSUTMII Technical Specifications. These samples were then analyzed for the ^{128}I gamma-ray photopeak using a Canberra Series 80 Multichannel Analyzer (MCA) and the germanium lithium-drifted detector system number one (Ge(Li)1) at the Kansas State University Neutron Activation Analysis facility. This system is shown in Fig. 4.3. The multichannel analyzer was operated with a coarse grain of 100, a fine grain of 3.0, and shaping set at 3. The pileup rejector was off, the input polarity was positive, the gate was off, and the baseline was set at 4.76. The analyzer was in the peak height analysis mode, the ADC IN was set for the amplifier, and the memory of the CRT was set for 2048 channels. The live count time was set at 400 seconds and the calibration equation was $0.934 \text{ keV/channel} + 7.787$. The lower discrimination level of the MCA's single channel analyzer was set at 0.3, while the upper discrimination level was at 10.0.

The resulting gamma-rays from the activated ^{128}I decay, from each sample vial were then counted on the Ge(Li)1 detector. This detector has a full width at half maximum of 2.37 keV for ^{60}Co , 1332 keV gamma rays. The adsorbent column samples were placed upright upon a bremsstrahlung cap that was positioned on top of the detector while counting. A diagram of this counting configuration is shown in Fig. 4.4. The bremsstrahlung cap was used in this case to filter out the beta particles associated with the chlorine in the resin, discussed in

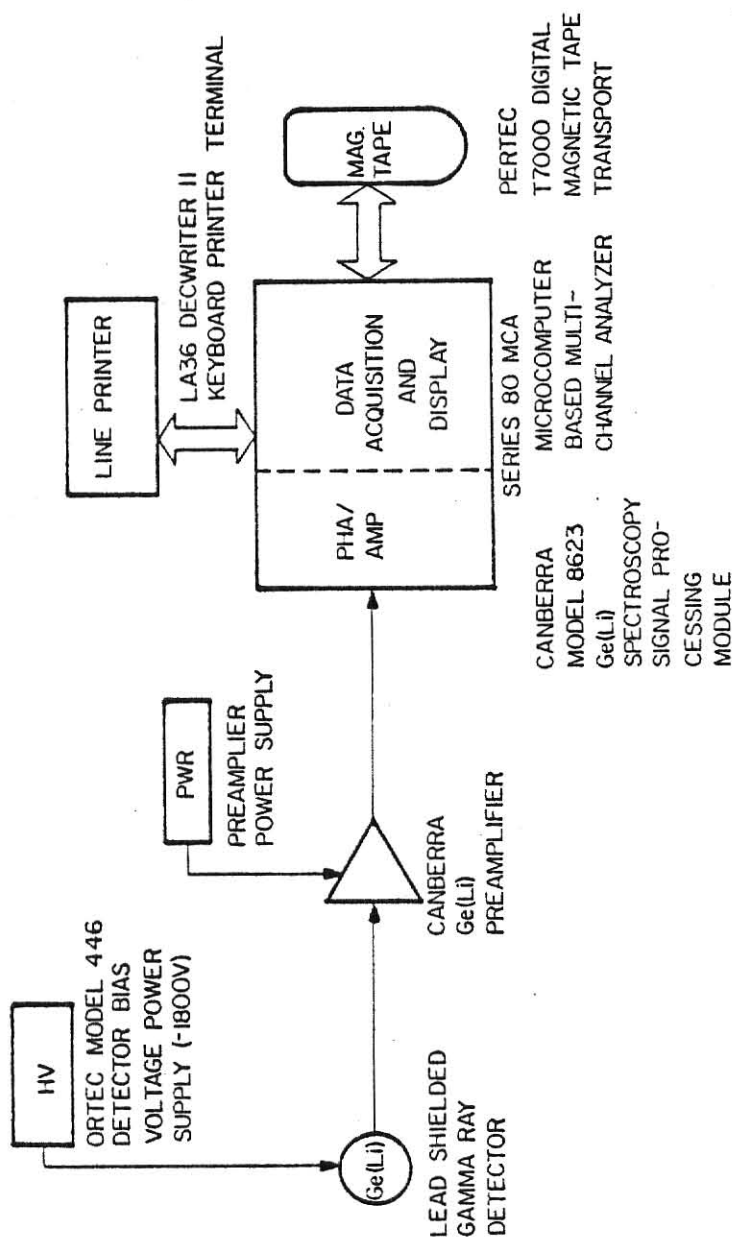


Fig. 4.3. The Canberra Series 80 Multichannel Analyzer and the Germanium Lithium-drifted detector system used for data collection after sample irradiation.

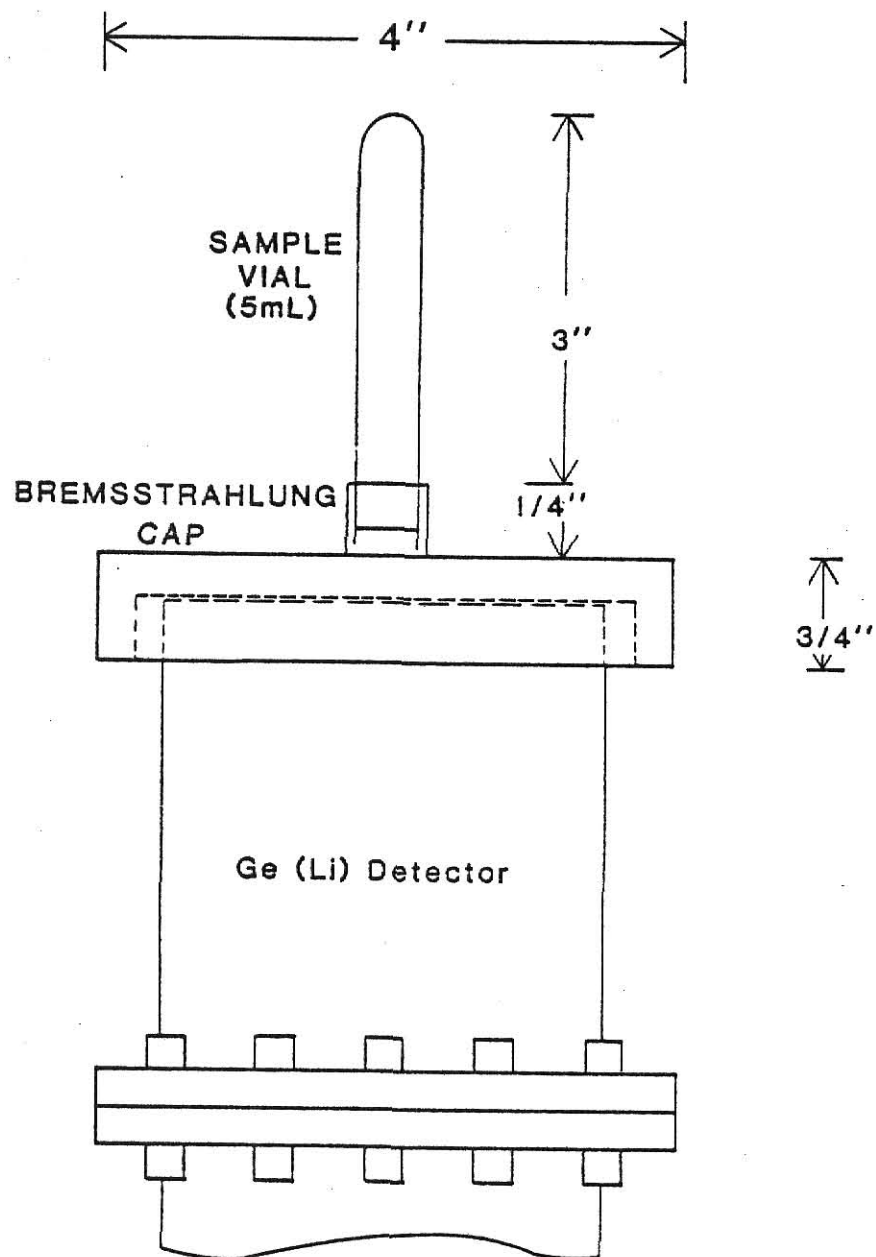


Fig. 4.4. The configuration used for counting the resulting gamma rays from the activated ^{128}I present in the sample vials.

Section 3.6, and the ^{128}I decay. Also, to insure that the counting geometry remained constant the bremsstrahlung cap remained in place even while analyzing the charcoal adsorbent column samples. However, no bremsstrahlung cap was needed for counting the ^{56}Mn gamma rays resulting from the activated iron wire flux monitors, which were used to correct for neutron flux variations using the method described in Section 3.1. These iron wire flux monitors were analyzed by counting the ^{56}Mn gamma rays for 400 seconds upon the center of the detector.

Using the energy calibration equation, $0.934 \text{ keV/channel} + 7.787$ found using a known NBS source, the ^{128}I gamma-ray photopeak occurred at channel number 466 and the region of interest for this peak was set from 437.6 keV to 448.8 keV on channel numbers 460 to 472. The region of interests were selected so that the photopeak area was maximized while the error (based on counting statistics, and computed by the Series 80 MCA) was minimized. Also, for the iron wire flux monitor, the ^{56}Mn gamma-ray photopeak occurred at channel number 898 and the region of interest was set from 836.6 keV to 858.1 keV or channel numbers 887 to 910.

Once the gamma rays were counted for 400 seconds for each column sample, each column's pulse height distribution was placed on magnetic tape. A computer program, described in the theory section of this thesis, was then used to subtract the chlorine component from these pulse height distributions. After this subtraction, the ^{128}I photopeak area was calculated, corrected for decay time, corrected for neutron flux variations using the ^{56}Mn gamma-ray photopeak area, and finally used to determine the collection efficiencies of the adsorbent columns.

4.5 Standard Curve

In order to determine the amount of iodine collected on each column, standard curve data were obtained. The procedure for this was to place varying amounts of solid iodine into five vials, each containing 4 ml of resin. The amounts of iodine varied from 0.0010 g to 0.0215 g. These masses were weighed using the Mettler Balance. After insuring that the contents of the vials were homogeneously mixed, they were then heat sealed and wrapped with an iron wire flux monitor. These samples were then irradiated at 10 kw for 2.5 minutes in KSUTMII RSR. Analysis of these samples was done in the same manner as was described in the preceeding sections. The counting rate (counts per second), due to ^{128}I , of each sample was then plotted versus the mass of iodine placed in each sample. The resulting graph is the relationship between the sample ^{128}I counting rate and iodine mass. Using a least squares line fit on these data establishes the relationship between the measured ^{128}I counting rate and the unknown mass of iodine. Hence, the amount of iodine in the columns may be determined from the ^{128}I counting rate.

4.6 Experimental Conditions Investigated

In the following experimental conditions that were investigated, each individual study was conducted inside a laboratory hood so that the surrounding conditions could be easily controlled. Each study was chosen because pertinent literature²¹ indicated that the chosen parameters--temperature, air flow rate, incident mass of iodine, and humidity--were fundamental to designing an adsorption column.

4.6.1 Temperature

The first parameter chosen for study in this thesis was temperature. In a laboratory or nuclear reactor location, temperature cannot always be controlled. Thus, it is important that an adsorbent work efficiently under varying temperatures. Therefore, temperatures were varied inside the experimental hood and column efficiencies were found for the corresponding experimental temperatures.

The temperature study was conducted by first using a Fisher Infa-Radiator heat lamp and Master model HG 501 heat gun to elevate the temperature in the hood. The resin and charcoal beds were then filled and packed tight between the two column end screens. The charcoal filter paper was placed in the filter holder and the system was assembled. Next, 0.02 g of solid iodine (I_2) was placed in the iodine reservoir and the pump was started. Air was passed through the system until all the iodine sublimed. The columns were then prepared for irradiation as indicated in Section 4.2, also the equipment was rinsed as indicated above. This study was done at temperatures of 23, 31, 40 and 50°C under the same above described conditions, for both an "A" column of resin and charcoal.

4.6.2 Air Flow Rate

Air flow rate was chosen for the second study because of its impact on efficiency. In the case of organic iodides, efficiency may vary substantially with flow rate.

The flow rate study was then conducted at nominally 23°C. Again, the resin and charcoal beds were packed tight between the column end

screens, a charcoal filter was placed in the filter holder and the system was assembled. Then, 0.02 g of solid iodine was placed in the iodine reservoir and the pump was started.

The pump was run until all the iodine had sublimed, and passed into the system. The columns were then prepared for irradiation and the equipment was rinsed as in the temperature experiments. The study was done at flow rates of 10, 15, 20, 25, and 30 l/min, which were varied by turning the flow rate adjusting screw at the pump. The study was done for both an "A" column of resin and charcoal.

4.6.3 Retention

For the third study, the retention of iodine with exposure to varying temperatures was selected. If radioiodine was not retained under varying temperatures, this could prove hazardous to persons in the vicinity of the adsorption column.

An iodine retention study for both charcoal and resin was conducted at temperatures ranging from 120 to 200°C. The procedure used was to first place 0.02 g of solid iodine into 10 sample vials. Five samples contained 4 ml of resin, and the other five contained 4 ml of charcoal. These samples were then irradiated after being mixed to insure homogeneity, heat sealed, and wrapped with an iron wire flux monitor. The samples were counted on the MCA as before so that the ^{128}I counting rate of the samples before heating could be found. After allowing for each of the radioisotopes to safely decay, the charcoal and resin samples were each heated in a Thermolyne, Type 10500, oven for 30 minutes at 120, 140, 160, 180, and 200°C, respectively. These samples

were then prepared for irradiation as indicated above. After irradiation the samples were again counted on the MCA so that the ^{128}I counting rate of the samples after heating could be found. The ratio, ^{128}I counting rate after heating $\times 100 / ^{128}\text{I}$ counting rate before heating, represented the percent of iodine loss due to heating.

4.6.4 Incident Mass of Iodine

Another study selected was to vary the mass of iodine in the column. Under normal operating conditions, only very small amounts of iodine are collected in adsorption columns. However, during a crisis nuclear situation, larger quantities of iodine may suddenly be released and collected in these adsorption columns. The effect of larger amounts of iodine in these columns on efficiency was therefore examined.

The procedure used for this study was the same as those described earlier except that this study was conducted at nominally 23°C and at a constant flow rate of 25 l/min. Also, the mass of iodine which was sublimed varied from 0.0102 to 0.1010 g for both an "A" column of resin and one of charcoal.

4.6.5 Humidity

In order to study the effect of humidity on the efficiency of iodine adsorption, for both resin and charcoal, another system was designed and assembled from polypropylene. This system is shown in Fig. 4.5. Humidity was selected for examination since it is so inconsistent under natural circumstances. In this study, the worst humidity case, that of having the column saturated by water, was examined. This was done by varying the amount of iodine incident on an "A" column of wet resin and on an "A" column of wet charcoal immersed in 4 ml of distilled

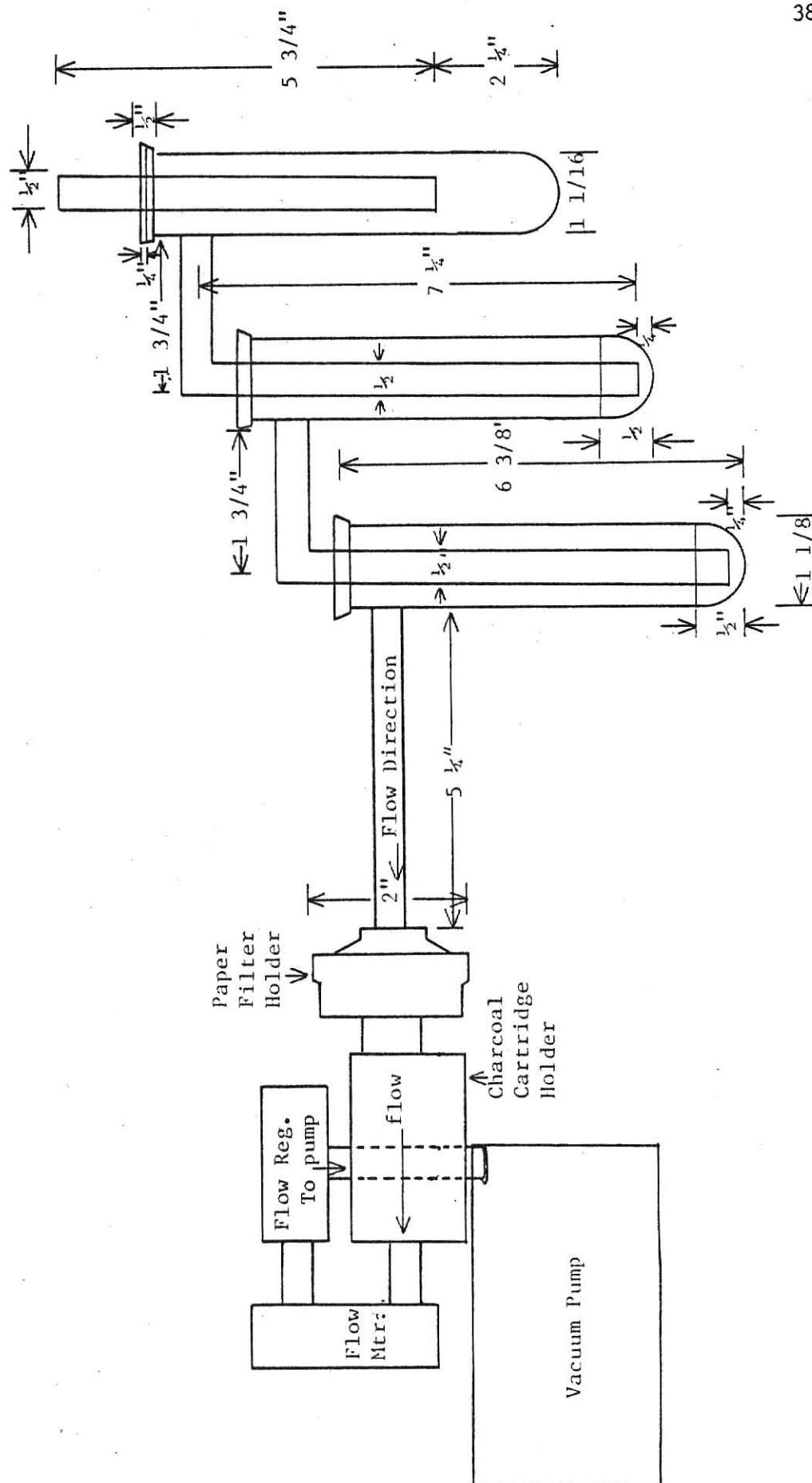


Fig. 4.5. The iodine sampling system used for the humidity study, illustrating the dimensions and location of each of the system's components.

water. The "B" column, as before, contained 4 ml of resin, although in this study it was saturated with water and immersed in 4 ml of distilled water. The study was done at a nominally 23°C and at a flow rate of 10 l/min.

The mass of iodine incident on the columns varied from 0.005 g to 0.024 g. After all the iodine placed in the reservoir had sublimed, the pump was disengaged and the columns were prepared for irradiation as before. The procedure for analyzing the samples and rinsing the equipment were the same as those used in earlier studies.

4.6.6 Radon and Thoron Collection

The final study selected for examination was the effect of radon and thoron adsorption in the charcoal and resin adsorption columns. This study was chosen in order to determine whether or not the resin would adsorb naturally occurring radon and thoron. It was hoped that this study would show that the resin would not collect radon and thoron, and thus would make a better iodine air sampler than charcoal.

The procedure used in this study was to first place 40 ml of resin and 40 ml of charcoal into two separate cartridges. These cartridges were cylindrical in shape, constructed of polypropylene, with stainless steel, fine mesh screens attached at each end of the cartridge. These cartridges were then each placed on an air sampler, and air was drawn through them for 3-5 days. Environmental conditions during the 3-5 day period were overcast, with low cloud cover after a rainfall. These meteorological conditions were ideal for radon collection. After this period, the cartridges were removed from the air samplers and the mesh screens replaced with uncontaminated mesh screens. The samples were

then placed upon the Ge(Li)1 detector, with the surface that was exposed to the atmosphere nearest the detector surface. Any resulting gamma rays from naturally occurring radon or thoron daughter product decay were then counted for 5000 seconds. The resulting gamma-ray photopeaks were then identified.

The second experiment in this study was to replace the screens with filter papers and repeat the above described experiment. However, in this case, any resulting gamma rays from naturally occurring radon or thoron daughter product decay collected on the filter paper would also be counted for 5000 seconds. Any resulting gamma photopeaks would then be identified.

5.0 RESULTS AND CONCLUSIONS

5.1 Mass of Iodine Collected

The relationship between the ^{128}I counting rate and the mass of iodine collected is defined to be the standard curve. This relationship can be found by measuring the counting rate (counts/s) of the samples. This counting rate results from the 442.9 keV gamma ray produced by the decaying ^{128}I . A plot of the measured counting rate versus the mass of iodine (g) in the respective samples yields the graph shown in Figure 5.1. Applying a least squares line fit to these data resulted in the following linear relationship between the measured counting rate C and the unknown mass M of the iodine,

$$C = 60045.3 M - 0.5. \quad (5.1)$$

The unknown mass of iodine present in a given sample can be determined by measuring the counting rate, resulting from the gamma-ray decay of ^{128}I , and by applying Equation (5.1).

5.2 Elevated Temperature

The temperature study was performed to compare the efficiencies of the resin and the charcoal adsorption columns operated under the same conditions at various ambient temperatures. The results of this study are listed in Table 5.1. From these data, the conclusion can be drawn that, for an air flow rate of 25 l/min, and for the mass of iodine collected up to 0.02 g, the temperature of the iodine-air stream did not affect the efficiency of either the resin or the charcoal columns. The minimum efficiency, which occurred for charcoal adsorption of iodine, was 99.7.

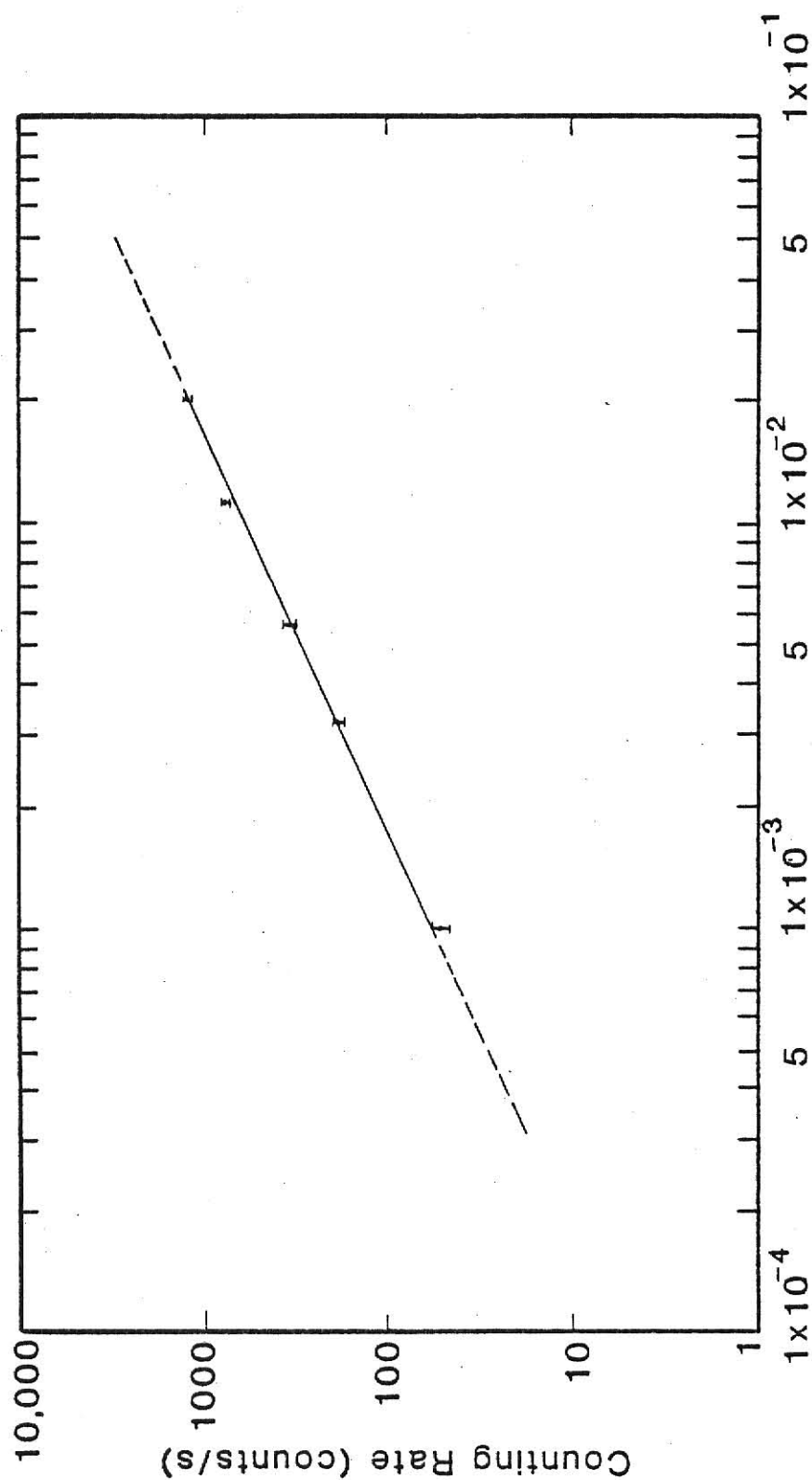


Fig. 5.1. Graph of the linear relationship between the measured sample counting rate resulting from the ^{128}I gamma-ray decay, and the iodine mass present in the sample.

Table 5.1 Experimental data for adsorption column collection efficiencies, for both resin and charcoal, at varying temperatures.

Ambient Temperature (°C)	Column Efficiency (%)	
	Resin	Charcoal
23	99.9 ± 3.8	100.0 ± 3.0
31	99.9 ± 3.4	99.9 ± 3.2
40	100.0 ± 2.8	99.7 ± 3.4
50	100.0 ± 3.2	99.9 ± 3.8

5.3 Air Flow Rate

Iodine adsorption efficiencies of resin and charcoal columns were investigated as a function of air flow rate. This study was conducted at nominally 23°C with 0.02g of iodine collected on the columns. As shown in Table 5.2, air flow rates ranged from 10 l/min to 30 l/min for both resin and charcoal adsorption columns. The resulting collection efficiencies, under these conditions, were greater than or equal to $99.7 \pm 3.9\%$. Hence, the conclusion that variations in air flow rate, in the range studied, will not affect the efficiency of either of the adsorption columns is acceptable.

5.4 Mass of Incident Iodine

The incident iodine mass study was designed to study the effect, on collection efficiencies, of flowing varying amounts of iodine through resin and charcoal columns. It was expected that the efficiencies of both the columns would be initially constant and possibly greater than 99.9%, but that the efficiencies of the columns would decrease as the mass of iodine incident on the column increased. However, as shown in Table 5.3, the point that this would occur (breakthrough) was not reached in this study. The range of the mass of iodine incident on the column was from 0.0102g to 0.1010g. The study was conducted at an air flow rate of 25 l/min and a nominal temperature of 23°C. Under these conditions, the results are that the efficiencies of the two columns, resin and charcoal, are equivalent and at least equal to $99.7 \pm 5.7\%$. Therefore, the conclusion that variations in the incident mass of iodine, for the range studied, will not affect the collection efficiency of either adsorption column is valid.

Table 5.2. Experimental data for adsorption column collection efficiencies, for both resin and charcoal, at varying flow rates.

Air Flow Rate (l/min)	Column Efficiency (%)	
	Resin	Charcoal
10	100.0 \pm 3.9	100.0 \pm 3.0
15	100.0 \pm 3.3	100.0 \pm 3.6
20	99.9 \pm 3.1	100.0 \pm 3.6
25	99.9 \pm 3.2	100.0 \pm 3.8
30	100.0 \pm 5.2	99.7 \pm 3.9

Table 5.3. Experimental data for resin and charcoal adsorption column efficiencies for various incident iodine masses.

Mass of Iodine Incident on Resin Column (g)	Column Efficiency (%)
0.0102	99.7 \pm 5.7
0.0231	100.0 \pm 4.4
0.0296	100.0 \pm 4.5
0.0567	99.9 \pm 3.8
0.0570	99.9 \pm 2.8
0.0587	99.9 \pm 2.9
0.0874	100.0 \pm 2.6
Mass of Iodine Incident on Charcoal Column (g)	Column Efficiency (%)
0.0125	100.0 \pm 2.7
0.0128	100.0 \pm 3.0
0.0284	99.9 \pm 3.0
0.0515	100.0 \pm 2.6
0.0650	99.9 \pm 2.7
0.0799	99.9 \pm 2.6
0.1010	100.0 \pm 2.7

5.5 Post Collection Heating

The ability of the resin and the charcoal to retain iodine at elevated temperatures was examined in this study. Both charcoal and resin, each with 0.02g of iodine adsorbed to them, were exposed for 30 minutes to temperatures varying from 120°C to 200°C. The results of this temperature study are shown in Table 5.4. In the retention study of charcoal, the conclusion drawn was that, under the temperature range studied, very little iodine was removed by heating, even at the highest temperatures. However, this study was conducted under static conditions (no air flow across the adsorbent). Under flow conditions, the results may be very dependent of temperature. The results of the resin study were inconclusive. This was due to the fact that as the resin was heated the individual beads would shrink. Hence, the volume of the resin changed, resulting in a change in the detector counting geometry and thus producing unreliable results.

5.6 High Humidity

The study of the effect of humidity on the efficiency of iodine adsorption for both resin and charcoal columns was examined by varying the amount of iodine incident (0.005g to 0.024g) on the column, at a nominal temperature of 23°C, and an air flow rate of 10 l/min. The humidity condition examined was the worst operating humidity case, that of having the column saturated by water. These results, shown in Figure 5.2 for the charcoal columns, did not vary significantly. However, the moisture did degrade the charcoal collection efficiency from $97.3 \pm 3.1\%$ to $97.1 \pm 3.3\%$. Resin column results, shown in Figure 5.3, were disappointing since the moisture significantly degraded the collection

Table 5.4. Experimental data for the retention of adsorbed iodine on resin or charcoal at various temperatures.

Temperature (°C)	$\frac{{}^{128}\text{I Counting Rate After Heating}}{{}^{128}\text{I Counting Rate Before Heating}} \times 100\%$	
	Resin	Charcoal
200	109.6 ± 3.3	97.1 ± 2.6
180	107.3 ± 3.5	96.8 ± 2.7
160	105.7 ± 3.9	99.3 ± 3.0
140	109.7 ± 4.9	98.0 ± 3.3
120	105.4 ± 5.3	103.2 ± 3.6

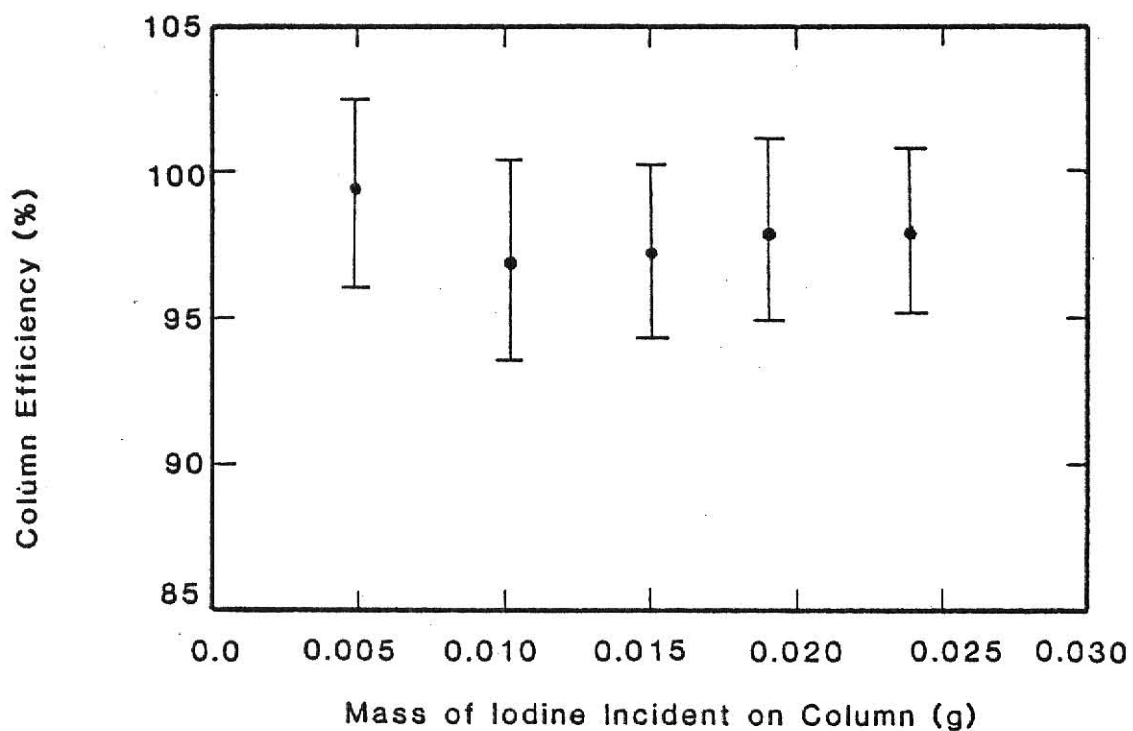


Fig. 5.2. Charcoal adsorption column efficiency versus the mass of iodine incident on the column, under high humidity conditions (columns saturated with water).

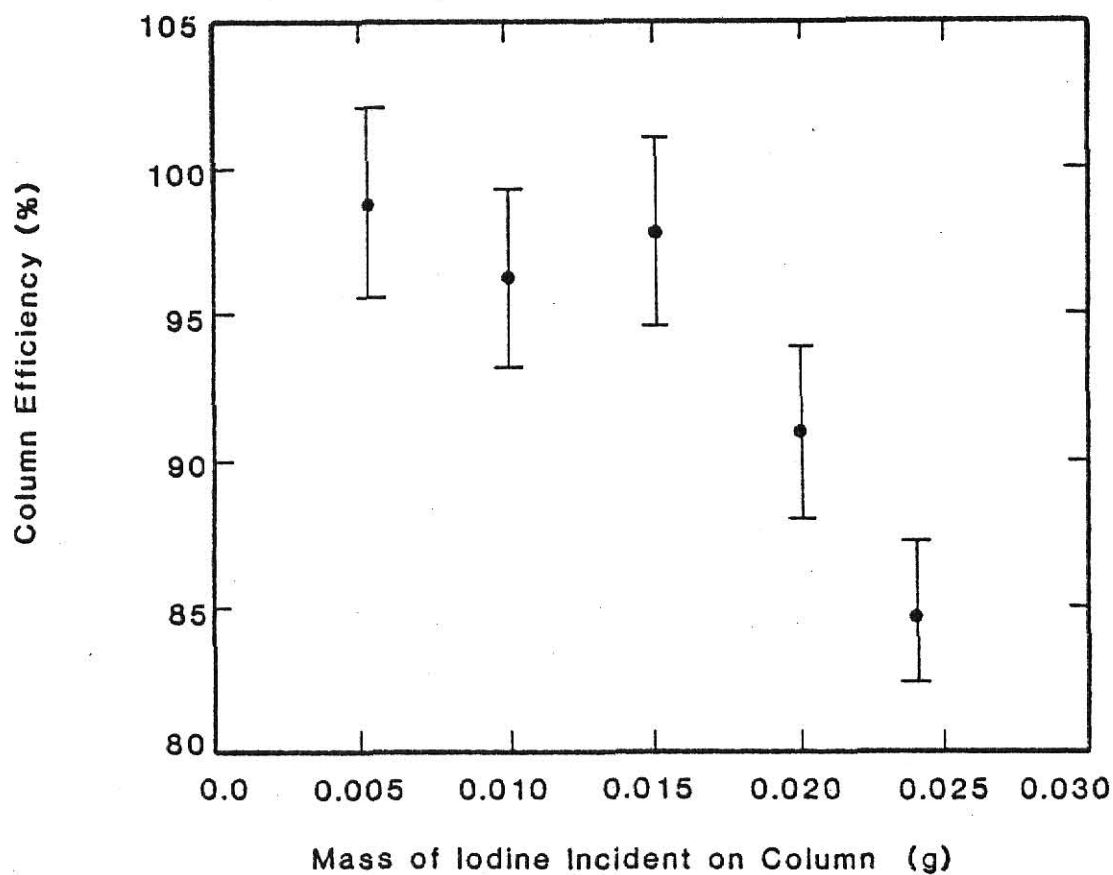


Fig. 5.3. Resin adsorption column efficiency versus the mass of iodine incident on the column, under high humidity conditions (columns saturated with water).

efficiency of the column. Thus, unless a column is to be used with incident masses of iodine below 0.0053g impregnated charcoal is the better choice for an iodine adsorption column under high humidity conditions.

5.7 Radon and Thoron Collection

The radon and thoron collection study was performed with the hope that the resin would be a better iodine air sampler than charcoal and would not collect other radionuclides, such as radon and thoron. The results of the radon and thoron collection study were obtained through two experiments. In the first experiment, air was simultaneously drawn through a resin and a charcoal adsorption cartridge. Neither the resin cartridge nor the charcoal cartridge contained a particulate filter. The second experiment was similar to the first, except in this case, both the resin and charcoal cartridges contained a particulate filter.

The results of the first experiment showed that for both the resin and charcoal cartridge, thoron daughter products were found in the adsorbent material and on the cartridge wire screen exposed to the atmosphere. However, from these data no conclusion can be drawn as to whether or not there is an advantage to using charcoal or resin since both collected particulate thoron daughter products.

The thoron daughter products, mentioned in the preceding paragraph, were found to be particulate in form from the results of the second experiment. When a particulate filter was used, no radon or thoron daughter products were found in the adsorbent material of either resin or charcoal. However, thoron daughter products were found on the filter

papers (See Figure 5.4). This indicated that the thoron daughter products are in particulate form and/or are attached to dust particles.

At the KSUTMII nuclear reactor, the problem described in section 1.0, where the charcoal filter paper collected radon and thoron daughter products and triggered the iodine monitor alarm is due to the particulate filter paper not the charcoal. This conclusion is based on the results of the second experiment. One possible solution would be to place a particulate filter in front (upstream) of the charcoal filter. However, both the particulate filter and the charcoal filter must be monitored, since radioiodine may exist in either particulate or vapor form.

5.8 Conclusion Summary

From the studies conducted, it was determined that, in general, resin and charcoal are comparable air samplers for iodine monitors, exhibiting a nominal efficiency of 100%. Exception were the cases of high humidities and cost comparison, where the charcoal was the better air sampling material.

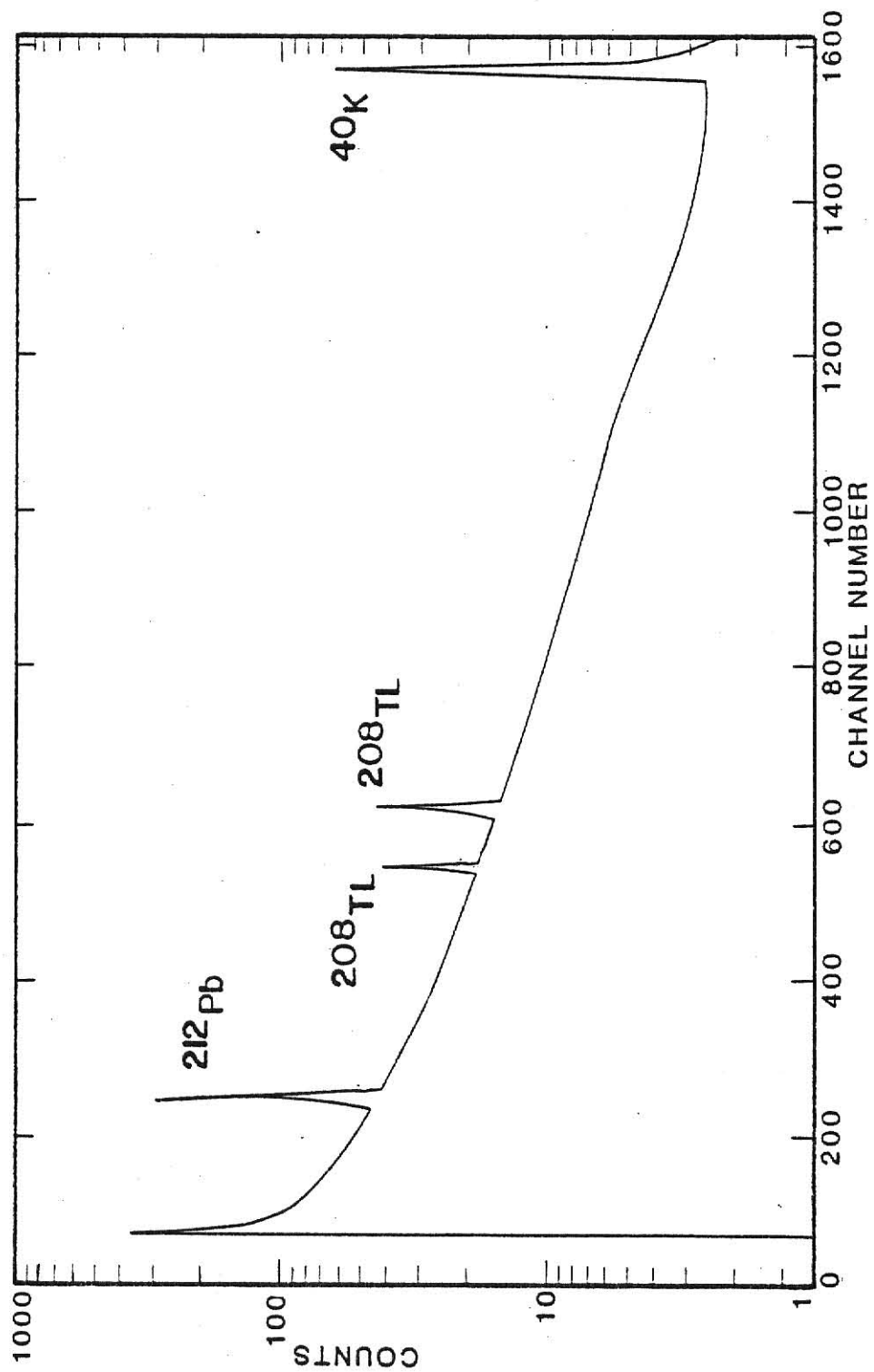


Fig. 5.4. Pulse height distribution resulting from gamma-ray decay of thoron daughter products collected on the particulate filter papers.

6.0 RECOMMENDATIONS

A number of recommendations, based upon the results of the research reported in this thesis, are now provided.

The first recommendation concerns the development of a mathematical model to describe the operation of the resin adsorption column. One approach would be to use the exchange zone method.²² In this method, an exchange zone is defined as the region within the column where the concentration of iodine in the air-iodine gas mixture is reduced from 95% to 5% of the initial concentration. This zone first forms at the beginning of the column. As additional iodine is collected within the resin column, the resin in the first zone becomes saturated and the zone moves down the column to a new position. Zone transitions will continue to occur at a constant velocity provided the iodine concentration remains constant for a given temperature and flow rate. Hence, knowing the length of the column and the velocity at which the zone penetrates the column, the time required for the iodine to pass completely through the column can be found. Therefore, the column will only provide efficient iodine collection until this calculated time. This model could then be used to calculate the optimal size of the column. A good indication that this model actually applies, to the resin columns investigated, occurred during data collection. A zone was actually observed to be moving through the column.

Recommendations involving experimental techniques are the development of: a variable humidity study, experiments using differing molecular forms and compounds of iodine, and a detector system that is more efficient. As described in more detail below, the completion of

each of these recommendations would improve the overall assessment of the applicability of the resin to radioiodine collection in laboratories and at nuclear power plants.

A variable humidity study would allow the efficiencies of resin and charcoal to be compared over a wide range of humidities. This recommendation is based upon the experimental results showing that at high humidity conditions, i.e., the column being saturated with water, resin and charcoal efficiencies showed a marked difference. The charcoal's performance was much better at high iodine levels. However, at lower iodine levels, the performance was equivalent for charcoal and resin. Perhaps data measured at different humidities will explain this disparity of efficiencies at higher iodine levels.

The study involving differing molecular forms and compounds of iodine arises from the fact that the radioiodine in the gaseous effluents³, from a nuclear power plant, may be in several forms other than elemental iodine (I_2). These may be inorganic iodides, principally HOI, and organic iodides, predominately CH_3I . In order to determine whether or not the resin adsorbs these forms, experimental studies involving both organic and inorganic forms of iodine must be undertaken.

A more efficient gamma-ray detector should be selected for further study of this resin. This detector system would allow measurement of smaller quantities of iodine. This would allow investigations to be performed at typical concentrations of radioiodine existing at both nuclear power plants and in laboratories utilizing radioiodine. The desirability of developing a laboratory instrument for routine monitoring of radioiodine could then be established.

7.0 ACKNOWLEDGEMENTS

The author would like to express his thanks to Dr. Gale G. Simons for his help during the experimental stage and most especially for his outstanding review of this thesis. Much appreciation is offered to Jack Higginbotham and Tim DeBey for their help and advice during this research. Special thanks are extended to the Kansas State University Nuclear Engineering Department for their financial support. The author is also grateful to Barbara Wielczka, for her drafting work.

Finally, the author would like to thank Mr. & Mrs. Ronald Cazel, whose financial and moral support are greatly appreciated, and also his wife Carma, for her help and encouragement.

8.0 REFERENCES

1. C. Pelletier, E. Barefoot, J. Cline, and W. Emel, "Radioiodine Source And Other Radionuclide Effluent Measurements At Nuclear Power Plants:", Electric Power Research Institute, NP-101 (Jan. 1976).
2. V. C. Furtado, T. J. Kneip and M. Eisenbud, "Measurement of Low Levels of Iodine-131 in Reactor Atmospheres", Nucl. Appl. Techn. 9,268-273 (Aug., 1970).
3. P. G. Voilleque, "Iodine Species in Reactor Effluents and in the Environment", Electric Power Research Institute, NP-1269 (Dec. 1979).
4. Hassler, J. W. Purification with Activated Charcoal, (Chemical Publishing Company, New York, 1974).
5. RadeCo/SAI, 4060 Sorrento Valley Blvd., San Diego, California, 9212, Price List, May 1, 1980.
6. J. E. Cline, "Retention of Noble Gases by Silver Zeolite Iodine Samplers", Science Applications, Inc. Report, 1980.
7. B. Sansoni, "Specific Molecular Adsorption of Iodine on Anion Exchangers", Angew, Chem. 73, 493 (1961).
8. A. V. Nikolaev, V. L. Bogatyrev, S. I. Sokolova, and A. I. Vulikh, "Sorption of Iodine Vapors on Anion-Exchange Resins Under Dynamic Conditions", Dok. Akad. Nauk. SSSR, Proceedings, Section: Chemistry 167, 841-843 (1966).
9. Lambert, J. P., "Biological, Chemical and Physical Properties of a Triiodinated Resin Column", Ph.D. Dissertation, Kansas State University, 1975.
10. J. E. Browning, K. Banerjee and W. E. Reisinger, "Airborne Concentration of I-131 in a Nuclear Medicine Laboratory", J. Nucl. Med. 19, 1078-1081 (1978).
11. L. Lefever, Dow Chemical Company, Midland, Michigan (Private Communication).
12. A. Wheeler, "Reaction Rates and Selectivity in Catalyst pores", Advances in Catalysis, Volume III (Academic Press, Inc., New York, 1951), p. 253.
13. Ibid, p. 258.
14. Data Sheet, Scott Health and Safety Products, South Haven, Michigan, 1981.

15. R. R. Bellamy, "Elemental Iodine and Methyl Iodide Adsorption of Activated Charcoal at Low Concentration", Nucl. Safety 15, 712 (Dec. 1974).
16. R. E. Adams, R. D. Ackley, and R. P. Shields, "Application of Impregnated Charcoals for Removing Radioiodine From Flowing Air at High Relative Humidity", Treatment of Airborne Radioactive Wastes, Proceedings, I.A.E.A., Vienna, 387 (1968).
17. A. R. Foster, and R. L. Wright, Jr., "Basic Nuclear Engineering" (Allyn and Bacon, Inc., Boston, Massachusetts, 1977), p. 205.
18. C. A. Pelletier, E. D. Barefoot, J. E. Cline, R. I. Hemphill, W. A. Emel, and P. G. Voilleque, "Sources of Radioiodine at Boiling Water Reactors", Electric Power Instituts, NP-495 (Feb. 1978), pp. A.76-A.85.
19. G. Shortley, and D. Williams, Elements of Physics, (Prentice Hall, Inc. Englewood Cliffs, New Jersey, 1971), p. 367.
20. R. W. Clack, J. R. Fagan, W. R. Kimel, and S. Z. Mikhail, Kansas State University TRIGA Mark II Reactor Hazards Summary Report, Special Report No. 7, 1961.
21. T. Vermeulen, G. Klein, and N. K. Hiester, "Adsorption and Ion Exchange", Chemical Engineers' Handbook, 5th ed. (McGraw-Hill Book Company, New York, 1973), pp. 16.12-16.21.
22. Michaels, A. S. "Simplified Method of Interpreting Kinetic Data in Fixed-Bed Ion Exchange", Ind. Eng. Chem. 44, 1922-30 (1952).

APPENDIX A: STANDARD DEVIATION DERIVATIONS

The equation used to calculate the standard deviation of the total number of counts within the gamma-ray photopeak area is derived by using the standard propagation of error technique which is (Glen F. Knoll, Radiation Detection and Measurement, (Wiley, New York, 1979), p. 131)

If R is a function of N independent variables

q_i , $i=1, \dots, N$, each of which has a standard deviation σ_i , then

(writing $R = f(q_1, q_2, \dots, q_N)$) the standard deviation of R is

$$\sigma^2(R) = \sum_{i=1}^N (\partial R / \partial q_i)^2 \sigma_i^2 \quad (A.1)$$

In order to calculate the standard deviation of the ^{128}I gamma-ray photopeak area after subtraction of the chlorine component, discussed in Section 3.6, Eq. (A.1) was then applied to the equations in the program CL-SUBT. In program FDC, Eq. (A.1) was used to calculate the standard deviation for the counting rate, corrected for neutron flux variations and decay times, resulting from each adsorption column's ^{128}I gamma-ray photopeak. Equation (A.1) was also applied to Eq. (3.22) in Section 3 to determine the standard deviation for each column's calculated collection efficiency.

Spectrum 1A is defined as the pulse height spectrum for the irradiated resin samples which did not contain iodine, i.e., virgin resin. A representation of a typical spectrum is shown in Fig. A.1. Spectrum 1B is the spectrum obtained by measuring the pulse height distribution corresponding to the gamma-ray emission of the resin sample which contains iodine (See Fig. A.2). General terms, related to the

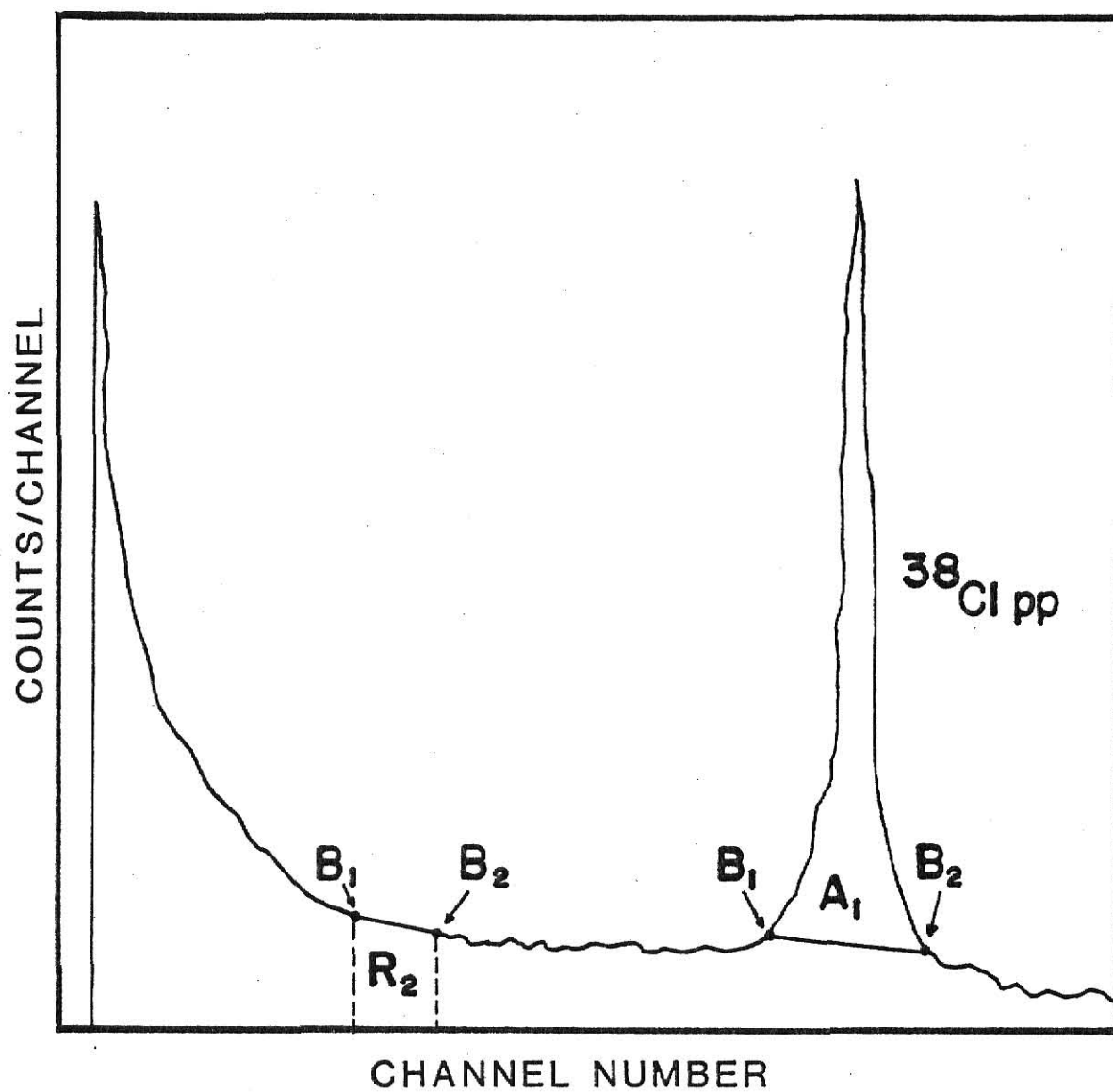


Fig. A.1. Representation of a typical pulse height spectrum for an irradiated resin sample which did not contain iodine.

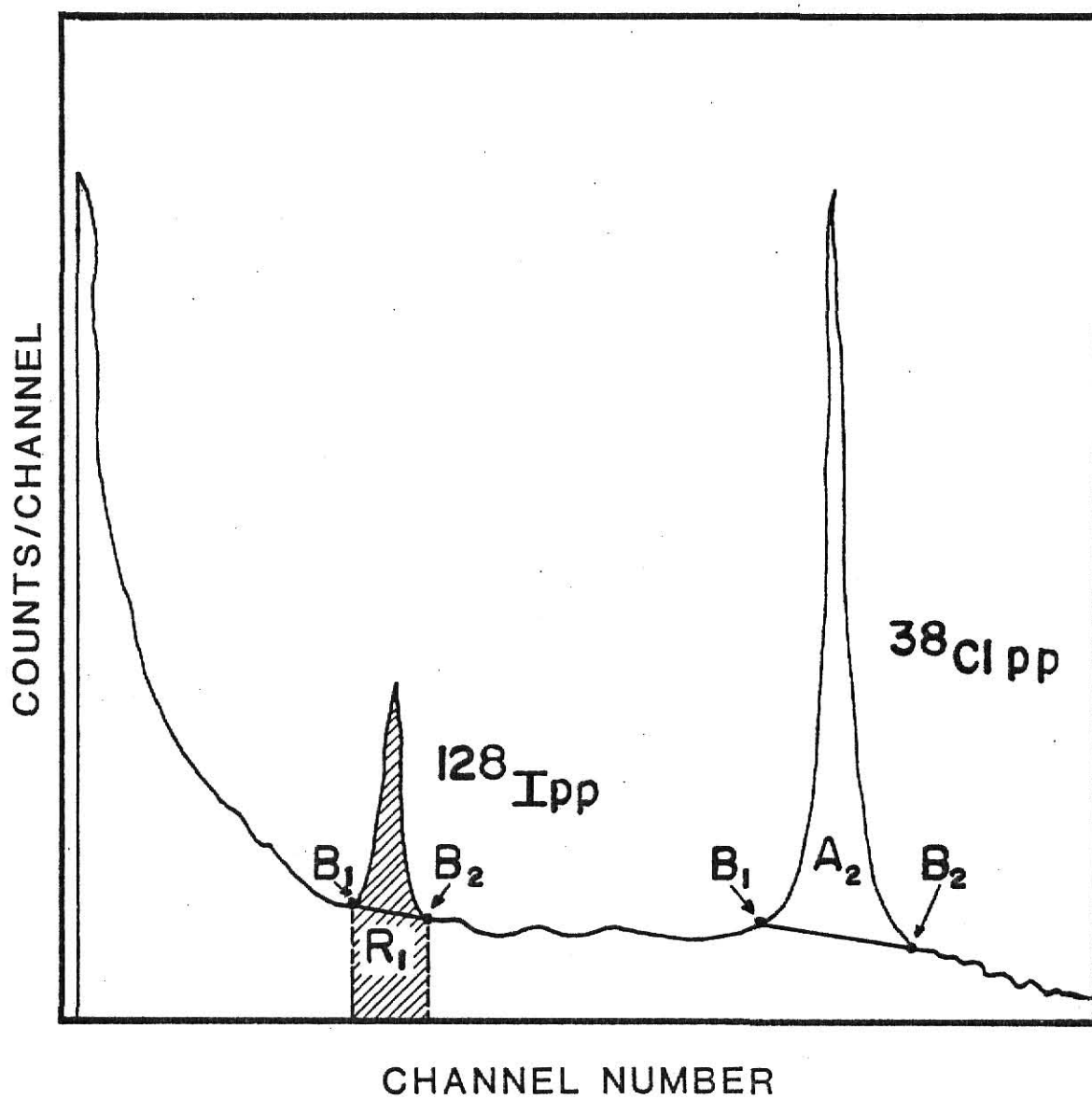


Fig. A.2. Illustration of the pulse height distribution for an irradiated resin sample containing iodine.

pulse height data, used to derive the desired equations are defined as follows:

T \equiv the total number of counts in the iodine region of interest (ROI) after subtraction of the chlorine component.

A \equiv area of the iodine gamma-ray photopeak after subtraction of the chlorine component.

R_1 \equiv the total number of counts in the iodine ROI of spectrum 1B.

R_2 \equiv the total number of counts in the iodine ROI of spectrum 1A.

A_2 \equiv the gamma-ray photopeak area in the chlorine ROI of spectrum 1B.

A_1 \equiv the gamma-ray photopeak area in the chlorine ROI of spectrum 1A.

NORM \equiv the normalization factor, A_2 / A_1 , that accounts for different decay times and neutron flux variations between data sets.

F \equiv the total normalization factor ($0.9 \times \text{NORM}$). This is used to prevent the subtraction of too much background between spectra 1A and 1B.

Therefore, subtracting the background spectrum from the spectrum of interest yields

$$T = R_1 - FR_2. \quad (\text{A.2})$$

Using Eq. (A.1) and $\text{NORM} = A_2 / A_1$ gives

$$\sigma^2(\text{NORM}) = \left(\frac{1}{A_1}\right)^2 \sigma_{A_2}^2 + \left(-\frac{A_2}{(A_1)^2}\right)^2 \sigma_{A_1}^2. \quad (\text{A.3})$$

Then, from radiation counting statistics and Eq. (A.1), the variance of A_1 is given by

$$\sigma^2(A_1) = \sigma^2(\text{ROI}_{\text{chlorine}}) + \left(\frac{N}{2}\right)^2 [\sigma^2(B_1) + \sigma^2(B_2)]$$

or

$$\sigma^2(A_2) = (\sqrt{\text{INT}})^2 + \left(\frac{N}{2}\right)^2 [(\sqrt{B_1})^2 + (\sqrt{B_2})^2],$$

where

INT \equiv the total number of counts in ROI before subtraction of the chlorine component,

B_1 \equiv the average background count immediately before the ROI,

B_2 \equiv the average background count immediately after the ROI, and

N \equiv the number of channels in the ROI.

Similarly,

$$\sigma^2(A_2) = \sigma^2(\text{ROI}_{\text{chlorine}}) + \left(\frac{N}{2}\right)^2 [\sigma^2(B_1) + \sigma^2(B_2)]$$

or

$$\sigma^2(A_2) = (\sqrt{\text{INT}})^2 + \left(\frac{N}{2}\right)^2 [(\sqrt{B_1})^2 + (\sqrt{B_2})^2] .$$

Letting $B = 0.9 \times \text{NORM} \times R_2$, and using Eq. (A.1) yields

$$\sigma^2(B) = (0.9R_2)^2 \sigma^2(\text{NORM}) + (0.9 \text{ NORM})^2 \sigma^2(R_2) , \quad (\text{A.4})$$

where $\sigma^2(\text{NORM})$ is given by Eq.(A.3) and

$$\sigma^2(R_2) = \sigma^2(\text{INT}) = (\sqrt{\text{INT}})^2 .$$

Now, applying Eq. (A.1) to Eq. (A.2) results in

$$\sigma^2(T) = (1)^2 \sigma^2(R_1) + (-1)^2 \sigma^2(B) , \quad (\text{A.5})$$

where $\sigma(B^2)$ is given by Eq. (A.4) and

$$\sigma^2(R_1) = \sigma^2(\text{INT}) = (\sqrt{\text{INT}})^2 .$$

After the subtraction of the chlorine component, applying Eq. (A.1) to the area calculation yields

$$\sigma^2(A) = \sigma^2(T) + \left(\frac{N}{2}\right)^2 [\sigma^2(B_1) + \sigma^2(B_2)]$$

or

$$\sigma^2(A) = \sigma^2(T) + \left(\frac{N}{2}\right)^2 [(\sqrt{B_1})^2 + (\sqrt{B_2})^2] , \quad (\text{A.6})$$

where $\sigma^2(T)$ is given by Eq. (A.5) .

Applying the correction for decay and neutron flux variations, derived in Section 3.1, yields

$$A_o = \frac{A}{400_s} e^{\lambda_I t_I} \left[\frac{A_{wref} M_w}{A_w M_{wref}} e^{-\lambda_w (t_w - t_{wref})} \right], \quad (A.7)$$

where

A_o = the initial iodine count rate,

λ_I = the decay constant for ^{128}I ,

t_I = the iodine decay time,

A_{wref} = the reference iron wire, ^{56}Mn , gamma-ray
photopeak area,

M_{wref} = the reference iron wire mass,

A_w = the iron wire, ^{56}Mn , gamma-ray photopeak area,

M_w = the iron wire mass,

λ_w = the decay constant for ^{56}Mn ,

t_w = the iron wire decay time, and

t_{wref} = the reference iron wire decay time.

Applying Eq. (A.1) to Eq. (A.7) gives the variance for A_o ,

$$\begin{aligned} \sigma^2(A_o) = & \left[\frac{A}{400 \text{ s}} e^{\lambda_I t_I} \frac{A_{wref} M_w}{A_w M_{wref}} e^{-\lambda_w(t_w - t_{wref})} \right]^2 [\sigma^2(A) \left(\frac{1}{A}\right)^2 + \lambda_I \sigma^2(t_I) \\ & + \left(\frac{1}{A_{wref}}\right)^2 \sigma^2(A_{wref}) + \left(\frac{1}{M_w}\right)^2 \sigma^2(M_w) + \left(\frac{1}{A_w}\right)^2 \sigma^2(A_w) + \left(\frac{1}{M_{wref}}\right)^2 \sigma^2(M_{wref}) \\ & + \lambda_w^2 \sigma^2(t_w) + \lambda_w^2 \sigma^2(t_{wref})] , \end{aligned} \quad (A.8)$$

where $\sigma^2(A)$ is given by Eq. (A.6) , and

$$\begin{aligned} \sigma^2(t_I) &= (0.0167)^2 \\ \sigma^2(A_{wref}) &= (\sqrt{A_{wref}})^2 , \\ \sigma^2(M_w) &= (0.0001)^2 , \\ \sigma^2(A_w) &= (\sqrt{A_w})^2 \\ \sigma^2(M_{wref}) &= (0.0001)^2 , \\ \sigma^2(t_w) &= (0.0167)^2 , \text{ and} \\ \sigma^2(t_{wref}) &= (0.0167)^2 . \end{aligned}$$

The efficiency E of a column (See Section 3.7) is given by

$$E = \left(1 - \frac{A_o \text{ in "B" cartridge}}{A_o \text{ in "A" cartridge}} \right) \times 100\% . \quad (A.9)$$

Applying Eq. (A.1) to Eq. (A.9) results in

$$\begin{aligned} \sigma^2(E) = & \left(\frac{1}{A_o \text{ in "A" cartridge}} \right)^2 (\sigma^2(A_o \text{ in "A" cartridge}) \\ & + \sigma^2(A_o \text{ in "B" cartridge})) + \left(- \frac{A_o \text{ in "A" cartridge} - A_o \text{ in "B" cartridge}}{(A_o \text{ in "A" cartridge})^2} \right)^2 \\ & (\sigma^2(A_o \text{ in "A" cartridge})) , \end{aligned} \quad (A.10)$$

where $\sigma^2(A_o)$ is given by Eq. (A.8) .

Finally, the variance of the counting rate ratio, count rate after heating / count rate before heating, used in the temperature retention study (See Section 4.6.3) is

$$\begin{aligned} \sigma^2(\text{ratio}) = & \left(\frac{1}{A_o \text{ before heating}} \right)^2 \sigma^2(A_o \text{ after heating}) \\ & + \left(- \frac{(A_o \text{ after heating})}{(A_o \text{ before heating})^2} \right)^2 \sigma^2(A_o \text{ before heating}) , \end{aligned} \quad (A.11)$$

where $\sigma^2(A_o)$ is given by Eq. (A.8).

Appendix B

CL-SUBT List

This Appendix contains a listing of the Fortran WATFIV computer program, CL-SUBT. This program was used to subtract the chlorine component from the experimental pulse height distributions.

```

$JCB
//      TIME=(1,00)
/*TAPE800
/*TAPE9
//TIM EXEC PGM=IEBGNER
//SYSPRINT DD SYSOUT=A
//SYSUT1 DD UNIT=TAPE800,VOL=SER=NAAL11,DISP=SHR,
//      LABEL=(1,NL,,IN),DCB=BLKSIZE=1542
// DD UNIT=AFF=SYSUT1,VOL=(,RETAIN,SER=NAAL11),
// LABEL=(2,NL,,IN),DCB=BLKSIZE=1542
// DD UNIT=AFF=SYSUT1,VOL=(,RETAIN,SER=NAAL11),
// LABEL=(3,NL,,IN),DCB=BLKSIZE=1542
// DD UNIT=AFF=SYSUT1,VOL=(,RETAIN,SER=NAAL11),
// LABEL=(4,NL,,IN),DCB=BLKSIZE=1542
// DD UNIT=AFF=SYSUT1,VOL=(,RETAIN,SER=NAAL11),
// LABEL=(5,NL,,IN),DCB=BLKSIZE=1542
//SYSUT2 DD UNIT=TAPE1600,VOL=(PRIVATE,RETAIN),
// DSN=&&TRM,DISP=(NEW,PASS),DCB=(BLKSIZE=1542)
//SYSIN DD DUMMY
//FORT EXEC FORTGCLG
//FORT.SYSIN DD *
C ***** CL-SUBT *****
C *
C *      WRITTEN BY J. K. SHULTIS (6/77).
C *      REVISED BY J. F. HIGGINBOTHAM (7/80)
C *      REVISED BY D. G. GREEN (10/80)
C *
C *      CL-SUBT MAY BE USED TO REMOVE GAMMA SPECTRA FROM A MAGNETIC
C *      TAPE GENERATED BY THE CANBERRA SERIES 80 MULTICHANNEL
C *      ANALYZER. THIS CODE WILL THEN SUBTRACT THE CHLORINE COMPONENT
C *      FROM THE GAMMA SPECTRA AND PRINT THE RESULTING SPECTRA.
C *      IT WILL ALSO CALCULATE PHOTOPEAK AREAS AND STANDARD DEVIATIONS
C *      USING PROPAGATION OF ERRORS.
C *
C *      THE FIRST SPECTRUM, SPECTRUM 1, IS FROM AN IRRADIATED
C *      BLANK RESIN SAMPLE AND HENCE CONTAINS ONLY THE CHLORINE
C *      PHOTOPEAK. THE FOLLOWING SPECTRA ARE THOSE FROM WHICH THE
C *      CHLORINE COMPONENT IS TO BE SUBTRACTED.
C *
C *      EACH SPECTRUM REQUIRES TWO INPUT DATA CARDS.
C *      IF MORE THAN ONE SPECTRUM IS TO BE PUNCHED, PRINTED OR
C *      PLOTTED, THEN WITH EACH ADDITIONAL SPECTRUM THE FOLLOWING
C *      TWO JCL CARDS MUST BE PLACED BEHIND THE LABEL CARD AS FOLLOWS:
C *      //      LABEL=(1,NL,,IN),DCB=BLKSIZE=1542
C *
C *      ADD THESE CARDS
C *      // DD UNIT=AFF=SYSUT1,VOL=(,RETAIN,SER=NAAGGS),
C *      // LABEL=(2,NL,,IN),DCB=BLKSIZE=1542
C *
C *      REMEMBER TO INCREMENT THE LABEL NUMBER FOR MORE THAN 2 SPECTRA
C ***** INPUT DATA *****
C *

```

PLT00002

PLTCC003

PLT00004

PLT00005

PLT00007

PLT00014

PLT00015

PLT00016

PLT00018

PLT00019

PLT00020

PLT00021

PLT00022

PLT00023

PLT00028

PLT00029

PLT00030

PLT00031

PLT00032

PLT00033

PLT00034

PLT00035

PLT00036

PLT00037

PLT00038

PLT00039

PLT00040

PLT00041

PLT00042

PLT00046

PLT00047

PLT00048

PLT00049

```

C *      EACH SPECTRUM REQUIRES TWO DATA CARDS. THE FIRST CARD FORMAT
C *      IS (I4,I2). THE SECOND CARD FORMAT IS (3I4). THE FOLLOWING
C *      QUANTITIES ARE SPECIFIED ON THE FIRST CARD:
C *
C *      NCHNLS = NUMBER OF CHANNELS IN THE SPECTRUM
C *      NPRINT = 0 IF NO PRINT OUT OF SPECTRUM IS DESIRED
C *              = 1 IF PRINT OUT OF SPECTRUM IS DESIRED
C *
C *      THE SECOND CARD DEFINES THE QUANTITIES:
C *
C *      I      = 1 FOR THE IODINE PHOTOPEAK
C *      I      = 2 FOR THE CHLORINE PHOTOPEAK
C *      MIN(I) = THE MINIMUM CHANNEL NUMBER OF THE REGION OF
C *              INTEREST
C *      MAX(I) = THE MAXIMUM CHANNEL NUMBER OF THE REGION OF
C *              INTEREST
C *      K(I)   = THE NUMBER OF ENDCPTS IN THE REGION OF INTEREST
C *
C *      DEFINITION OF OTHER QUANTITIES:
C *
C *      ID      = SPECTRUM NUMBER
C *      I      = 1 FOR IODINE PHOTOPEAK
C *      I      = 2 FOR CHLORINE PHOTOPEAK
C *      J      = SPECTRUM NUMBER
C *      A(I,J)  = PHOTOPEAK AREA
C *
C *      I      = CHANNEL NUMBER OF SPECTRUM
C *      J      = SPECTRUM NUMBER
C *      SPECT(I,J) = SPECTRUM BEFORE SUBTRACTION CONTAINING
C *                  INTEGER VALUES
C *      NORM(J)  = NORMALIZATION FACTOR
C *      SPEC(I,J) = NORMALIZED SPECTRUM 1
C *      SPECR(I,J) = SPECTRUM BEFORE SUBTRACTION, PREVIOUS
C *                  INTEGER VALUES ARE NOW REAL VALUES
C *      SPEC(I,J) = SPECTRUM AFTER SUBTRACTION, CONTAINS REAL
C *                  VALUES
C *      KSPE(I,J) = SPECTRUM AFTER SUBTRACTION, PREVIOUS REAL
C *                  VALUES ARE NOW INTEGER VALUES, USED FOR
C *                  PRINTOUT PURPOSES ONLY
C *
C *      INT      = SUM OF THE VALUES IN EACH CHANNEL IN THE
C *                  REGION OF INTEREST(ROI)
C *
C *      I      = 1 FOR IODINE PHOTOPEAK ROI
C *      I      = 2 FOR CHLORINE PHOTOPEAK ROI
C *      J      = SPECTRUM NUMBER
C *      SIGAS(I,J) = STANDARD DEVIATION SQUARED OF PHOTOPEAK AREA
C *      SIGR(I,J)  = STANDARD DEVIATION SQUARED OF THE SUM OF
C *                  VALUES IN ROI, CONTAINING REAL VALUES
C *      SIGV(I,J)  = STANDARD DEVIATION SQUARED OF THE SUM OF
C *                  VALUES IN ROI, CONTAINING INTEGER VALUES
C *      SIGD(I,J)  = STANDARD DEVIATION SQUARED OF BACKGROUND
C *                  IN ROI, CONTAINING REAL VALUES
C *      SIGN(J)    = STANDARD DEVIATION SQUARED OF THE
C *                  NORMALIZATION FACTOR
C *      SIGB(J)    = STANDARD DEVIATION SQUARED OF THE
C *                  NORMALIZED SPECTRUM ROI

```

```

PLT00053
PLT00054
PLT00061
PLT00062
PLT00065
PLT00066
PLT00067

```

```
C *          SIGT(J) = STANDARD DEVIATION SQUARED OF THE SUM OF
C *          VALUES IN THE ROI AFTER SUBTRACTION OF THE
C *          CHLORINE COMPONENT
C *          SIGI(J) = STANDARD DEVIATION SQUARED OF THE PHOTOPEAK
C *          AREA AFTER SUBTRACTION OF THE CHLORINE
C *          COMPONENT
C *
C ***** PLT00070
C ***** PLT00071
C ***** PLT00072
C
C      DIMENSION A(2,5)
C      INTEGER ID,NCHNLS
C      REAL NORM(5),SPEC(2048,5)
C      INTEGER SPECT(2048,5),K(2),MIN(2),MAX(2)
C      REAL SPECR(2048,5)
C      DIMENSION KSPE(2048,5)
C      REAL INT
C      DIMENSION SIGT(5),SIGD(2,5)
C      DIMENSION SIGAS(2,5),SIGR(2,5),SIGN(5),SIGB(5),SIGI(5),SIGV(2,5)
C
C *** READ IN THE SPECTRUM
C
C 11 READ(5,99,END=24,ERR=23) NCHNLS,NPRINT
C 99 FORMAT(I4,I2)
C    IF(NPRINT.EQ.2) GO TO 22
C    DO 250 J=1,2
C      READ(5,700) MIN(J),MAX(J),K(J)
C 700 FORMAT(3I4)
C 250 CONTINUE
C    READ(8,98,END=24,ERR=23) ID,(SPECT(I,ID),I=1,NCHNLS)
C 98 FORMAT(I6,(I7,16(16I6)))
C
C ***** PLT00073
C
C ***CALCULATE THE CHLORINE PHOTOPEAK AREA AND THE STANDARD DEVIATION
C ***SQUARED OF THIS AREA
C
C      CALL AREA(SPECT,K,MIN,MAX,A,2,ID,NCHNLS,SIGAS,SIGV)
C
C ***PRINT THE CHLORINE PHOTOPEAK AREA AND THE STANDARD DEVIATION
C ***SQUARED
C
C      PRINT900,ID,A(2,ID)
C 900  FORMAT('O',4X,'CHLORINE AREA',I2,'=',E16.8)
C      PRINT1000,SIGAS(2,ID)
C 1000 FORMAT('O',4X,'STANDARD DEVIATION SQUARED OF CHLORINE AREA=',E16.8)
C 1)
C
C ***CALCULATE THE IODINE PHOTOPEAK AREA, TOTAL COUNTS IN THE REGION
C ***OF INTEREST, THE STANDARD DEVIATION SQUARED OF THIS AREA, AND OF
C ***THE IODINE REGION OF INTEREST
C
C      CALL AREA(SPECT,K,MIN,MAX,A,1,ID,NCHNLS,SIGAS,SIGV)
C      PRINT1001,ID,A(1,ID)
C 1001 FORMAT('O',4X,'IODINE AREA BEFORE SUBTRACTION OF SPECTRUM',I2,'=',E16.8)
C      PRINT1003,SIGAS(1,ID)
C 1003 FORMAT('O',4X,'STANDARD DEVIATION SQUARED OF IODINE AREA=',E16.8)
C      PRINT1002,ID,SIGV(1,ID)
C 1002 FORMAT('O',4X,'SIGMA**2 OF IODINE ROI OF SPECTRUM',I2,'=',E16.8)
```

```

C
C
C***PRINT OUT THE SPECTRUM BEFORE SUBTRACTION OF THE CHLORINE COMPONENT
C
      IF (NPRINT.EQ.0) GO TO 5
      WRITE(6,133) ID,NCHNLS,SPECT(1,ID)
133  FORMAT('1','SPECTRUM ID=',I4,5X,'SPECTRUM SIZE=',I5,5X,'COUNT TIME
      1(SEC)=' ,I6,/)
      WRITE(6,115)
115  FORMAT(2X,'CHNO',8X,'1',6X,'2',6X,'3',6X,'4',6X,'5',6X,'6',6X,
      1 '7',6X,'8',6X,'9',5X,'10',/)
      NLINES=(2048-1)/10.0
      DO 201 J=1,NLINES
      JJ=10*J-10
      JST=JJ+2
      JEND=JJ+11
201  WRITE(6,202) JJ,(SPECT(I,ID),I=JST,JEND)
202  FORMAT(2X,I4,2X,10I7)
      JJ=10*NLINES
      JST=JJ+2
      WRITE(6,202) JJ,(SPECT(I,ID),I=JST,NCHNLS)
      5 CONTINUE
      GO TO 11
C
C
C*** END OF PROGRAM OPTIONS
C
      22 WRITE(6,501)
      501 FORMAT('1 NORMAL END - BLANK DATA CARD ENCOUNTERED')
      DO 255 I=1,4
C
C***COMPUTE NORMALIZATION FACTORS AND THEIR STANDARD DEVIATIONS SQUARED
C
      NORM(I+1)=A(2,I+1)/A(2,1)
      SIGN(I+1)=((1/A(2,1))**2)*SIGAS(2,I+1)+(A(2,I+1)/A(2,1))**2**2*SIG
      1AS(2,1)
      SIGB(I+1)=((0.9*SIGV(1,1))**2)*SIGN(I+1)+((0.9*NORM(I+1))**2)*SIGV
      1(1,1)
C
C***PRINT NORMALIZATION FACTORS
C
      PRINT901,NORM(I+1)
901  FORMAT('0',4X,'NORM=',E16.8)
C
C***NORMALIZE BLANK RESIN SPECTRUM (CHLORINE COMPONENT)
C
      DO 260 J=1,NCHNLS
      SPEC(J,I+1)=NORM(I+1)*SPECT(J,1)
260  CONTINUE
255  CONTINUE
C
C***SUBTRACT NORMALIZED BLANK RESIN SPECTRUM FROM SPECTRA OF INTEREST
C
      DO 270 I=2,5
      DO 265J=1,NCHNLS
      SPECR(J,I)=SPECT(J,I)
      SPEC(J,I)=SPECR(J,I)-0.9*SPEC(J,I)

```

```

265  CONTINUE
      DO 10 III=1,NCHNLS
10    KSPE(III,I)=SPEC(III,I)
12    CONTINUE
C
C***PRINT OUT SPECTRUM AFTER SUBTRACTION OF CHLORINE COMPONENT
C
      WRITE(6,290) I,NCHNLS
290  FORMAT('1','SPECTRUM AFTER SUBTRACTION OF CHLORINE COMPONENT',5X,'
SPECTRUM ID=',I4,5X,'SPECTRUM SIZE=',I5)
      WRITE(6,291)
291  FORMAT(2X,'CHNO',8X,'1',6X,'2',6X,'3',6X,'4',6X,'5',6X,'6',6X,
1 '7',6X,'8',6X,'9',5X,'10',/)
      NLINES=(2048-1)/10.C
      DO 292 J=1,NLINES
      JJ=10*J-10
      JST=JJ+2
      JEND=JJ+11
292  WRITE(6,293) JJ,(KSPE(KK,I),KK=JST,JEND)
293  FORMAT(2X,I4,2X,10I7)
      JJ=10*NLINES
      JST=JJ+2
      WRITE(6,293) JJ,(KSPE(KK,I),KK=JST,NCHNLS)
C
C***CALCULATE IODINE PHOTOPEAK AREA AND STANDARD DEVIATION SQUARED
C***AFTER THE CHLORINE COMPONENT SUBTRACTION
C
      CALL REALA(SPEC,K,MIN,MAX,A,1,I,NCHNLS,SIGD,SIGR)
      SIGT(I)=SIGR(I,I)+SIGB(I)
      SIGI(I)=SIGT(I)+SIGC(I,I)
      PRINT275,I,A(1,I)
275  FORMAT('0',4X,'THE IODINE PHOTOPEAK AREA OF SPECTRUM',I2,' = ',E16
1.8)
      PRINT1275,SIGI(I)
1275 FORMAT('0',4X,'STANDARD DEVIATION SQUARED OF THE IODINE AREA=',E16
1.8)
C
C***COMPUTE THE CHLORINE PHOTOPEAK AREA AFTER THE CHLORINE COMPONENT
C***SUBTRACTION
C
      CALL REALA(SPEC,K,MIN,MAX,A,2,I,NCHNLS,SIGD,SIGR)
      PRINT280,I,A(2,I)
280  FORMAT('0',4X,'THE CHLORINE PHOTOPEAK AREA OF SPECTRUM',I2,' = ',E16
1.8)
270  CONTINUE
      GO TO 199
23  WRITE(6,502)
502  FORMAT('1 ERROR IN DATA ENCOUNTERED - JOB ABANDONNED')
      GO TO 199
24  WRITE(6,503)
503  FORMAT(' UNEXPECTEDLY RAN OUT OF DATA')
199  CONTINUE
      STOP
      END
      SUBROUTINE AREA(X,K,MIN,MAX,A,M,L,NN,SIGAS,SIGV)
C
C*** THIS SUBROUTINE CALCULATES THE PHOTOPEAK AREA FOR A GIVEN REGION

```

PLTC0132
PLT00133
PLTC0134
PLT00135
PLT00136
PLTC0137

PLT00142

C***OF INTEREST OF A SPECTRUM CONTAINING INTEGER VALUES. IT ALSO
 C***COMPUTES THE STANDARD DEVIATION SQUARED OF THE SUM OF THE VALUES
 C***IN THE REGION OF INTEREST, AND OF THE PHOTOPEAK AREA.

```

C
  REAL INT
  INTEGER K(M),MIN(M),MAX(M),MX,MN,C,X(NN,L)
  DIMENSION SIGAS(2,5),SIGV(2,5)
  DIMENSION A(2,5)
  C=K(M)
  MN=MIN(M)
  MX=MAX(M)
  N=MN+C-1
  J=MX-C+1
  SUM=0.0
  DO 215 I=MN,MX
    SUM=SUM+X(I,L)
215  CONTINUE
  INT=SUM
  SUM=0.0
  DO 220 I=MN,N
    SUM=SUM+X(I,L)
220  CONTINUE
  B=SUM/C
  SUM=0.0
  DO 225 I=J,MX
    SUM=SUM+X(I,L)
225  CONTINUE
  BI=SUM/C
  A(M,L)=INT-((B+BI)*0.5*(MX-MN+1))
  SIGV(M,L)=INT
  SIGAS(M,L)=INT+(((MX-MN+1)*0.5)**2)*(B+BI)
  RETURN
  END
  SUBROUTINE REALA(X,K,MIN,MAX,A,P,L,NN,SIGD,SIGR)

```

C
 C*** THIS SUBROUTINE CALCULATES THE PHOTOPEAK AREA FOR A GIVEN REGION
 C***OF INTEREST IN A SPECTRUM CONTAINING REAL VALUES. IT ALSO COMPUTES
 C***THE STANDARD DEVIATION SQUARED OF THE SUM OF VALUES IN THE REGION
 C***OF INTEREST, AND OF THE BACKGROUND IN THE REGION OF INTEREST.

```

C
  REAL X(NN,L),INT
  INTEGER K(M),MIN(M),MAX(M),MX,MN,C
  DIMENSION SIGD(2,5),SIGR(2,5)
  DIMENSION A(2,5)
  C=K(M)
  MN=MIN(M)
  MX=MAX(M)
  N=MN+C-1
  J=MX-C+1
  SUM=0.0
  DO 215 I=MN,MX
    SUM=SUM+X(I,L)
215  CONTINUE
  INT=SUM
  SUM=0.0
  DO 220 I=MN,N
    SUM=SUM+X(I,L)

```

```

220  CONTINUE
      B=SUM/C
      SUM=0.0
      DO 225 I=J,MX
      SUM=SUM+X(I,L)
225  CONTINUE
      BI=SUM/C
      A(M,L)=INT-((B+BI)*0.5*(MX-MN+1))
      SIGR(M,L)=INT
      SIGD(M,L)=(((MX-MN+1)*0.5)**2)*(B+BI)
      RETURN
      END

```

```

/*
//GO.FT08FO01 DD DSN=6&TRM,DISP=OLC
//GO.SYSIN DD *
$ENTRY
2048 1
  460 472  4
17391761  8
2048 1
  460 472  4
17391761  8
2048 1
  460 472  4
17391761  8
2048 1
  460 472  4
17391761  8
2048 1
  460 472  4
17391761  8
2048 2
/*

```

```

PLT00192
PLTCC193
PLT00194

```


Appendix C

FDC List

Contained in this Appendix is a listing of the Fortran WATFIV computer program, FDC. This program was used to correct the gamma-ray photopeak area for neutron flux variations and radioactive decay.


```

      TREF=197.2667
      DO 10 I=2,5
C
C***READ IN INPUT VALUES
C
      READ(5,100) MW,TW,AH,TI,AI,SIGI
100  FORMAT(2F10.5,2F10.3,2F10.1)
C
C***CALCULATE CORRECTED ACTIVITY
C
      A=((AI/400.0)*EXP(LAMI*TI)*(AREF/AH)*(MW/MREF)*EXP(-LAMW*(TW-TREF)
      1))
C
C***COMPUTE STANDARD DEVIATION SQUARED OF CORRECTED ACTIVITY
C
      SIGAS=A*A*((SIGI/(AI**2))+(LAMI**2)*(0.0167**2)+(1/AREF)+((1/MW)**
      12)*(0.0001**2)+(1/AH)+((1/MREF)**2)*(0.0001**2)+2*((LAMW**2)*(0.01
      167**2)))
      SIGAS=SIGAS**0.5
C
C***PRINT CORRECTED ACTIVITY AND STANDARD DEVIATION
C
      PRINT99,I
99  FORMAT('0',4X,'SPECTRUM ID=',I3)
      PRINT7,A
7   FORMAT('0',4X,'IODINE ACTIVITY=',E16.8)
      PRINT8,SIGAS
8   FORMAT('0',4X,'STANDARD DEVIATION OF IODINE ACTIVITY=',E16.8)
10  CONTINUE
      STOP
      END
$ENTRY
0.0874      83.633      10391.0      39.133      263.3      34258.2
0.0875      101.417      9527.0      52.417      392.4      24451.7
0.0850      121.933      8308.0      69.1      14668.9      42614.8
0.0874      134.383      8110.0      75.717      15813.5      61319.1
/*

```

Appendix D

Raw Data

This Appendix contains a series of tabular compilations of the raw data taken during the parameter studies of resin and charcoal iodine adsorbent materials.

Table D-I. Data for the reference iron wire
flux monitor.

Iron Wire Mass (g)	Iron Wire Decay Time (min)	⁵⁶ Mn Photopeak Area (counts)
0.0934	197.267	6299.0

Table D-II. Data for the standard curve, illustrating the relationship between the ^{128}I counting rate and the mass of iodine present in the sample.

Mass of Iodine in Sample (g)	Iron Wire Mass (g)	Iron Wire Decay Time (min)	^{56}Mn Photopeak Area (counts)	^{128}I Decay Time (min)	^{128}I Photopeak Area (counts)	^{128}I Counting Rate corrected for decay & flux variance (counts/s)
0.0010	0.0872	199.983	5325.0	123.5	625.7	52.4 ± 7.3
0.0032	0.0932	191.583	6441.0	111.15	3345.9	182.4 ± 13.5
0.0056	0.0932	186.25	6839.0	125.583	4458.4	349.9 ± 18.7
0.0124	0.0937	168.417	7555.0	144.0	5855.3	754.8 ± 27.5
0.0205	0.0876	219.05	4830.0	153.55	6629.3	1221.8 ± 39.9

Table D-III. Data showing the counting rate of the ^{128}I present on the resin before heating in the retention study.

Vial	Iron Wire Mass (g)	Iron Wire Decay Time (min)	^{56}Mn Photopeak Area (counts)	^{128}I Decay Time (min)	^{128}I Photopeak Area (counts)	^{128}I Counting Rate corrected for decay & flux variance (counts/s)
RI	0.0880	189.317	5862.0	113.317	22090.3	1341.6 ± 29.4
RII	0.0877	202.567	5677.0	129.9	13982.6	1304.4 ± 31.4
RIII	0.0915	215.38	5302.0	155.3	6832.0	1359.9 ± 39.1
RIV	0.0874	230.05	4898.0	170.05	4474.0	1298.4 ± 43.5
RV	0.0895	273.017	4247.0	187.75	3599.9	1663.1 ± 59.6

Table D-IV. Data showing the counting rate of ^{128}I present on the resin after heating in the retention study.

Temperature heated @ in °C	Vial	Iron Wire Mass (g)	Iron Wire Decay Time (min)	^{56}Mn Photopeak Area (counts)	^{128}I Decay Time (min)	^{128}I Photopeak Area (counts)	^{128}I Counting Rate corrected for Decay & Flux Variance (counts/s)
200	RI	0.0867	200.433	5498.0	92.433	43220.6	1470.3 ± 30.2
180	RII	0.0874	212.4	5399.0	106.9	28322.1	1400.2 ± 30.3
160	RIII	0.0874	224.333	4978.0	126.333	16487.9	1436.7 ± 34.1
140	RIV	0.0870	237.383	4834.0	159.55	6731.1	1424.8 ± 41.7
120	RV	0.0878	250.583	4517.0	183.75	4158.4	1753.2 ± 61.3

Table D-V. Data showing the counting rate of ^{128}I present on the charcoal before heating in the retention study.

Vial	Iron Wire Mass (g)	Iron Wire Decay Time (min)	^{56}Mn Photopeak Area (counts)	^{128}I Decay Time (min)	^{128}I Photopeak Area (counts)	^{128}I Counting Rate corrected for Decay & Flux Variance (counts/s)
CI	0.0871	159.767	6392.0	92.1	47765.6	1668.5 ± 32.2
CII	0.0871	176.533	5825.0	105.367	29174.1	1498.9 ± 30.9
CIII	0.0871	170.267	5679.0	119.1	20939.9	1518.8 ± 33.1
CIV	0.0862	203.033	5103.0	133.533	11168.4	1257.4 ± 31.2
CV	0.0877	215.95	5214.0	150.783	9989.1	1705.4 ± 43.1

Table D-VI. Data showing the counting rate of ^{128}I present on the charcoal after heating in the retention study.

Temperature heated @ ($^{\circ}\text{C}$)	Vial	Iron Wire Mass (g)	Iron Wire Decay Time (min)	^{56}Mn Photopeak Area (counts)	^{128}I Decay Time (min)	^{128}I Photopeak Area (counts)	^{128}I Counting Rate corrected for decay & flux variance (counts/s)
200	CI	0.0874	146.3	7493.0	80.467	70423.8	1619.7 ± 29.7
180	CII	0.0877	159.717	6719.0	93.217	42013.6	1450.3 ± 28.2
160	CIII	0.0875	149.733	6509.0	107.4	31477.0	1508.5 ± 31.5
140	CIV	0.0933	187.35	6547.0	125.833	14977.1	1232.5 ± 27.8
120	CV	0.0875	201.1	5704.0	145.433	12274.3	1760.7 ± 42.2

Table D-VII. Data collected during the humidity study
with resin as the adsorbent material.

Iodine Incident on Column (g)	128I Photopeak Area "A" Cartridge (counts)	128I Photopeak Area "B" Cartridge (counts)	128I Decay Time (min)	Iron Wire Mass (g)	⁵⁶ Mn Photopeak Area (counts)	Iron Wire Decay Time (min)	128I Counting Rate corrected for Decay & Flux Variance (counts/s)
0.0053	15813.5 -----	----- 392.4	75.717 52.417	0.0874 0.0875	8110.0 9527.0	134.383 101.417	310.7 ± 7.2 4.0 ± 1.6
0.0101	22095.4 -----	----- 1926.2	83.75 55.217	0.0851 0.0878	7058.0 8563.0	140.513 111.383	570.3 ± 12.6 22.6 ± 1.9
0.0152	15824.2 -----	----- 768.7	107.883 83.933	0.0878 0.0875	6686.0 7171.0	152.05 129.433	902.8 ± 20.7 21.9 ± 3.3
0.0201	17685.8 -----	----- 3185.3	115.25 89.367	0.0866 0.0875	6365.0 7026.0	162.583 134.867	1157.4 ± 25.9 105.3 ± 4.9
0.0238	35178.6 -----	----- 8185.9	81.8 66.533	0.0880 0.0875	7324.0 7676.0	140.8 128.367	886.4 ± 17.5 135.5 ± 4.0

Table D-VIII. Data collected during the humidity study
with charcoal as the adsorbent material.

Iodine Incident on Column (g)	¹²⁸ I Photopeak Area "A" Cartridge (counts)	¹²⁸ I Photopeak Area "B" Cartridge (counts)	¹²⁸ I Decay Time (min)	Iron Wire Mass (g)	⁵⁶ Mn Photopeak Area (counts)	Iron Wire Decay Time (min)	¹²⁸ I Counting Rate corrected for Decay & Flux Variance (counts/s)
0.0049	14668.9 -----	----- 263.3	69.1 39.133	0.0850 0.0874	8308.0 10391.0	121.933 83.633	240.8 + 5.3 1.8 ± 1.3
0.0102	10968.5 -----	----- 813.6	102.5 69.617	0.0876 0.0878	6808.0 7932.0	156.55 126.617	483.6 + 11.6 14.4 ± 2.1
0.0150	16152.1 -----	----- 1096.8	102.067 68.317	0.0873 0.0874	7186.0 7768.0	144.733 116.15	709.2 + 15.6 19.9 ± 2.5
0.0190	16602.0 -----	----- 876.9	106.55 72.8	0.0869 0.0873	6524.0 7473.0	153.55 120.3	870.1 + 19.5 18.3 ± 2.8
0.0238	26726.4 -----	----- 2348.3	99.983 49.783	0.0875 0.0867	6997.0 8150.0	155.817 115.283	1085.0 + 22.1 24.2 ± 1.8

Table D-IX. Data obtained during the elevated temperature experiment with the charcoal adsorbent material.

Temperature (°C)	Vial	Iron Wire Mass (g)	Iron Wire Decay Time (min)	⁵⁶ Mn Photopeak Area (counts)	¹²⁸ I Decay Time (min)	¹²⁸ I Photopeak Area (counts)	¹²⁸ I Counting Rate corrected for Decay & Flux Variance (counts/s)
23	C 23A	0.0851	168.367	6531.0	116.05	20174.6	1259.8 ± 26.9
	C 23B	0.0876	141.383	7227.0	90.55	0.0	0.0
31	C 31A	0.0867	190.8	6171.0	128.633	16172.6	1396.3 ± 31.3
	C 31B	0.0807	156.367	6407.0	103.867	13.3	0.6 ± 5.5
40	C 40A	0.0877	198.883	5659.0	134.217	12859.4	1379.1 ± 32.6
	C 40B	0.0869	155.5	7132.0	91.167	136.3	4.2 ± 4.4
50	C 50A	0.0871	212.067	5548.0	156.067	8108.1	1522.1 ± 40.4
	C 50B	0.0873	172.833	6585.0	118.333	30.1	2.0 ± 6.5

Table D-X. Data obtained during the elevated temperature experiment with the resin adsorbent material.

Temperature	Vial	Iron Wire Mass (g)	Iron Wire Decay Time (min)	⁵⁶ Mn Photopeak Area (counts)	¹²⁸ I Decay Time (min)	¹²⁸ I Photopeak Area (counts)	¹²⁸ I Counting Rate corrected for decay & flux variance (counts/s)
23	23A	0.0907	330.817	3247.0	122.483	16145.2	1249.8 + 33.5
	23B	0.0884	303.933	3594.0	88.433	29.6	0.9 + 6.4
31	31A	0.0898	317.183	3450.0	102.483	18979.8	1275.9 + 30.9
	31B	0.0917	287.083	4275.0	75.15	63.5	1.2 + 4.4
40	40A	0.0896	120.05	7531.0	99.05	32017.0	1414.1 + 28.4
	40B	0.0871	144.25	6921.0	70.25	0.0	0.0
50	50A	0.0894	136.067	7031.0	112.467	18425.6	1169.8 + 26.3
	50B	0.0895	138.417	7273.0	85.917	0.0	0.0

Table D-XI. Data obtained during the air flow rate study with the charcoal adsorbent material.

Flow Rate (L/min)	Vial	Iron Wire Mass (g)	Iron Wire Decay Time (min)	⁵⁶ Mn Photopeak Area (counts)	¹²⁸ I Decay Time (min)	¹²⁸ I Photopeak Area (counts)	¹²⁸ I Counting Rate corrected for Decay & Flux Variance (counts/s)
10	CF 10 A	0.0876	165.15	6675.0	113.983	22664.6	1365.6 ± 28.8
	CF 10 B	0.0931	139.483	7966.0	86.317	0.0	0.0
15	CF 15 A	0.0859	177.883	6125.0	139.217	9431.4	1154.9 ± 29.4
	CF 15 B	0.0894	152.65	7101.0	100.983	0.0	0.0
20	CF 20 A	0.0850	198.75	5373.0	132.1	9890.1	1019.5 ± 26.2
	CF 20 B	0.0931	162.283	6954.0	87.283	0.0	0.0
25	CF 25 A	0.0874	212.25	5255.0	146.25	7996.1	1210.3 ± 32.2
	CF 25 B	0.0858	184.117	5806.0	115.7	0.0	0.0
30	CF 30 A	0.0885	206.767	5874.0	151.433	6887.5	1117.4 ± 30.8
	CF 30 B	0.0872	172.867	6591.0	95.7	84.4	2.9 ± 4.9

Table D-XII. Data obtained during the air flow rate study
with the resin adsorbent material.

Flow Rate (L/min)	Vial	Iron Wire Mass (g)	Iron Wire Decay Time (min)	⁵⁶ Mn Photopeak Area (counts)	¹²⁸ I Decay Time (min)	¹²⁸ I Photopeak Area (counts)	¹²⁸ I Counting Rate corrected for Decay & Flux Variance (counts/s)
10	F 10 A	0.0874	179.383	5855.0	133.55	10039.8	1110.8 ± 30.5
	F 10 B	0.0873	193.017	5514.0	86.35	0.0	0.0
15	F 10 A	0.0854	132.5	7531.0	118,833	15967.1	1100.4 ± 25.9
	F 10 B	0.0845	143.3	7017.0	91.767	0.0	0.0
20	F 20 A	0.0864	137.917	7566.0	105,583	21311.9	999.7 ± 21.8
	F 20 B	0.0846	147.517	6765.0	76.183	0.0	0.7 ± 4.7
25	F 25 A	0.0885	138,167	7526.0	114.0	17868.1	1088.8 ± 24.5
	F 25 B	0.0883	155.2	6981.0	83.7	61.2	1.6 ± 5.3
30	F 30 A	0.0893	152.033	7149.0	129.2	6285.0	1003.5 ± 36.9
	F 30 B	0.0897	160.317	6661.0	86.8	0.0	0.0

Table D-XIII. Data collected which yielded the results of the incident iodine mass study with charcoal adsorbents.

Iodine Incident on Column (g)	Vial	Iron Wire Mass (g)	Iron Wire Decay Time (min)	^{56}Mn Photopeak Area (counts)	^{128}I Decay Time (min)	^{128}I Photopeak Area (counts)	^{128}I Counting Rate corrected for Decay & Flux Variance (counts/s)
0.0125	C5.41x10 ⁻⁵ AC C5.41x10 ⁻⁵ BC	0.0932 0.0878	148.0 117.55	7335.0 7086.0	63.467 72.55	48428.1 0.0	751.5 ± 14.4 0.0
0.0128	C5.96x10 ⁻⁵ AC C5.96x10 ⁻⁵ BC	0.0875 0.0861	145.3 139.333	6731.0 7150.0	92.467 82.167	21459.6 0.0	770.7 ± 16.6 0.0
0.0284	C5.78x10 ⁻⁵ AC C5.78x10 ⁻⁵ BC	0.0896 0.0878	165.083 135.683	6399.0 7315.0	116.25 87.35	24904.0 36.3	1705.3 ± 36.1 1.1 ± 4.6
0.0515	C5.23x10 ⁻⁵ AC C5.23x10 ⁻⁵ BC	0.0874 0.0932	143.717 116.033	7230.0 5646.0	98.05 70.867	78809.0 0.0	3094.5 ± 57.7 0.0
0.0650	C5.256x10 ⁻⁵ AC C5.256x10 ⁻⁵ BC	0.0877 0.0889	157.75 129.317	6481.0 8190.0	112.083 83.983	63974.0 13.9	3902.4 ± 74.7 0.4 ± 3.5
0.0799	C4.982x10 ⁻⁵ AC C4.982x10 ⁻⁵ BC	0.0878 0.0874	154.683 127.217	7156.0 7717.0	111.35 83.05	87350.3 157.6	4792.9 ± 88.4 4.1 ± 4.2
0.1010	C5.67x10 ⁻⁵ AC C5.67x10 ⁻⁵ BC	0.0874 0.0868	169.317 140.0	6572.0 7295.0	124.817 97.167	74924.4 0.0	6063.6 ± 114.6 0.0

Table D-XIV. Data obtained which yielded the results of the incident iodine mass study with resin adsorbents.

Iodine Incident on Column (g)	Vial	Iron Wire Mass (g)	Iron Wire Decay Time (min)	⁵⁶ Mn Photopeak Area (counts)	¹²⁸ I Decay Time (min)	¹²⁸ I Photopeak Area (counts)	¹²⁸ I Counting Rate corrected for Decay & Flux Variance (counts/s)
0.0102	3.98x10 ⁻⁵ AC 3.98x10 ⁻⁵ BC	0.0881 0.0874	198.0 216.167	5649.0 5236.0	140.833 112.0	4703.2 35.3	612.2 ± 23.9 2.0 ± 9.3
0.0231	4.76x10 ⁻⁵ AC 4.76x10 ⁻⁵ BC	0.0861 0.0867	185.183 205.967	6149.0 5081.0	161.35 125.8	6343.5 0.0	1386.7 ± 42.9 0.0
0.0296	3.86x10 ⁻⁵ AC 3.86x10 ⁻⁵ BC	0.0873 0.0896	197.167 208.85	4862.0 5034.0	166.167 134.183	5857.3 0.0	1778.7 ± 56.1 0.0
0.0567	5.78x10 ⁻⁴ AC 5.78x10 ⁻⁵ BC	0.0861 0.0806	192.55 202.783	5603.0 4572.0	180.383 145.783	8642.2 9.6	3400.8 ± 90.0 1.6 ± 17.73
0.0570	3.862x10 ⁻⁵ AC 3.862x10 ⁻⁵ BC	0.0895 0.0867	151.117 167.35	5977.0 5664.0	110.95 50.0	50851.9 1.9	3421.9 ± 67.5 0.1 ± 5.7
0.0587	4.86x10 ⁻⁵ AC 4.86x10 ⁻⁵ BC	0.0873 0.0888	142.35 161.3	6244.0 6292.0	128.85 97.63	32851.2 8.9	3526.3 ± 71.3 0.4 ± 6.9
0.0874	5.72x10 ⁻⁵ AC 5.72x10 ⁻⁵ BC	0.0875 0.0872	129.45 146.617	7900.0 7271.0	117.283 75.615	80284.1 0.0	5247.6 ± 95.5 0.0

COMPARISON STUDIES OF DOWEX MSA-1 RESIN AND SCOTT
IMPREGNATED CHARCOAL FOR IODINE ADSORBENTS
IN AN IODINE AIR MONITOR SYSTEM

by

DANIEL GEORGE GREEN

B.S., Kansas State University, 1980

AN ABSTRACT OF A MASTER'S THESIS

submitted in partial fulfillment of the
requirements for the degree

MASTER OF SCIENCE

Department of Nuclear Engineering

KANSAS STATE UNIVERSITY
Manhattan, Kansas

1981

ABSTRACT

A reasonable alternative to impregnated charcoal as an air sampler for an iodine monitor was examined. Impregnated charcoal is a collector of radionuclides such as xenon, as well as radioiodine. This collection of other radionuclides makes monitoring of radioiodine with charcoal difficult.

A study was undertaken to compare dehydrated Dowex MSA-1 resin to Scott triethylenediamine impregnated charcoal in order to determine which would be a better air sampler for an iodine monitor. Parameters examined in this research were elevated temperatures, air flow rates, mass of incident iodine, post collection heating, and high humidity. Each study was performed by allowing solid iodine to sublime and then be passed through an adsorption column of either resin or charcoal. The quantity of iodine collected on these columns was determined using neutron activation analysis. In this analysis, the columns were each irradiated in the Kansas State University TRIGA Mark II nuclear reactor. A neutron-gamma ray reaction produced ^{128}I from the stable ^{127}I collected in the column. Gamma-ray emissions from the ^{128}I were then counted using a germanium lithium-drifted detector and multichannel analyzer. From the counting rate data, measured for each of the columns, the column collection efficiency was found.

In a final study, air samplers were operated with resin and charcoal cartridges to determine whether charcoal and/or resin would

adsorb other radionuclides such as naturally occurring radon and thoron. After the air sampling was completed, the spectrometer system was used to measure any resulting gamma rays from naturally occurring radon or thoron daughter product decay.

From the studies conducted, it was determined that, in general, resin and charcoal are comparable air samplers for iodine monitors, exhibiting a nominal efficiency of 100%. Exception were the cases of high humidities and cost comparison, where the charcoal was the better air sampling material.